NAVAL POSTGRADUATE SCHOOL

MONTEREY, CALIFORNIA

THESIS

ADVANCED RESEARCH INTO IMAGING OF MOVING TARGETS

by

Chris Carroll

December 2009

Thesis Advisor: Brett Borden
Second Reader: Don Walters

Approved for public release; distribution is unlimited

REPORT DOCUMENTATION PAGE			Form Approved OMB No. 0704-0188
Public reporting burden for this collection of information is estimated to average 1 hour per response, including the time for reviewing instruction, searching existing data sources, gathering and maintaining the data needed, and completing and reviewing the collection of information. Send comments regarding this burden estimate or any other aspect of this collection of information, including suggestions for reducing this burden, to Washington headquarters Services, Directorate for Information Operations and Reports, 1215 Jefferson Davis Highway, Suite 1204, Arlington, VA 22202-4302, and to the Office of Management and Budget, Paperwork Reduction Project (0704-0188) Washington DC 20503.			
1. AGENCY USE ONLY ***(Leave blank)***	**2. REPORT DATE** December 2009	**3. REPORT TYPE AND DATES COVERED** Master's Thesis	
4. TITLE AND SUBTITLE Advanced Research into Imaging of Moving Targets		**5. FUNDING NUMBERS**	
6. AUTHOR(S) Chris Carroll			
7. PERFORMING ORGANIZATION NAME(S) AND ADDRESS(ES) Naval Postgraduate School Monterey, CA 93943-5000		**8. PERFORMING ORGANIZATION REPORT NUMBER**	
9. SPONSORING /MONITORING AGENCY NAME(S) AND ADDRESS(ES) N/A		**10. SPONSORING/MONITORING AGENCY REPORT NUMBER**	
11. SUPPLEMENTARY NOTES The views expressed in this thesis are those of the author and do not reflect the official policy or position of the Department of Defense or the U.S. Government.			
12a. DISTRIBUTION / AVAILABILITY STATEMENT Approved for public release; distribution is unlimited		**12b. DISTRIBUTION CODE**	

13. ABSTRACT (maximum 200 words)

Radar imaging is an area of tremendous interest as radar-based systems are perhaps the only all-weather, long range remote sensing systems. However, radar's continued utility and application in wide-ranging areas is fundamentally dependent on the ability to produce high-quality, artifact-free imagery. To date, the use of radar to identify and image moving objects remains of great interest. It is well known that motion in the scene gives rise to mispositioning or streaking when target motion is not properly addressed. Many techniques have been developed to handle moving objects, but these techniques typically make use of the *start-stop* approximation, in which a target in motion is assumed to be momentarily stationary while it is being interrogated by a radar pulse.

A new linearized imaging theory that combines the spatial, temporal and spectral aspects of scattered waves has been developed. This thesis studies the performance of this new imaging scheme. It also shows that the behavior of the imaging system is dependent on the aperture geometry and choice of radar waveforms transmitted.

14. SUBJECT TERMS Radar Imaging, Moving Targets, Point-Spread Function			**15. NUMBER OF PAGES** 73
			16. PRICE CODE
17. SECURITY CLASSIFICATION OF REPORT Unclassified	**18. SECURITY CLASSIFICATION OF THIS PAGE** Unclassified	**19. SECURITY CLASSIFICATION OF ABSTRACT** Unclassified	**20. LIMITATION OF ABSTRACT** UU

NSN 7540-01-280-5500 Standard Form 298 (Rev. 2-89)
Prescribed by ANSI Std. 239-18

THIS PAGE INTENTIONALLY LEFT BLANK

Approved for public release; distribution is unlimited

ADVANCED RESEARCH INTO IMAGING OF MOVING TARGETS

Christopher S. Carroll
Lieutenant Commander, United States Navy
B.S., US Merchant Marine Academy, 1993

Submitted in partial fulfillment of the
requirements for the degree of

MASTER OF SCIENCE IN APPLIED PHYSICS

from the

NAVAL POSTGRADUATE SCHOOL
December 2009

Author: Chris Carroll

Approved by: Professor Brett Borden
Thesis Advisor

Professor Donald Walters
Second Reader

Professor Andres Larazza
Chairman, Department of Physics

THIS PAGE INTENTIONALLY LEFT BLANK

ABSTRACT

Radar imaging is an area of tremendous interest as radar-based systems are perhaps the only all-weather, long range remote sensing systems. However, radar's continued utility and application in wide-ranging areas is fundamentally dependent on the ability to produce high-quality, artifact-free imagery. To date, the use of radar to identify and image moving objects remains of great interest. It is well known that motion in the scene gives rise to mispositioning or streaking when target motion is not properly addressed. Many techniques have been developed to handle moving objects, but these techniques typically make use of the *start-stop* approximation, in which a target in motion is assumed to be momentarily stationary while it is being interrogated by a radar pulse.

A new linearized imaging theory that combines the spatial, temporal and spectral aspects of scattered waves has been developed. This thesis studies the performance of this new imaging scheme. It also shows that the behavior of the imaging system is dependent on the aperture geometry and choice of radar waveforms transmitted.

THIS PAGE INTENTIONALLY LEFT BLANK

TABLE OF CONTENTS

I. INTRODUCTION....1
A. RADAR IMAGING....1
1. Radar Basics....2
2. Radar Measurables....3
B. SYNTHETIC APERTURE RADAR....4
1. System Parameters....4
2. Data Sampling....5
C. SAR IMAGING....6
1. Resolution....6
2. Radar Range Resolution for SAR....6
3. Radar Azimuthal Resolution for SAR....8
4. Stripmap SAR....8
5. Spotlight SAR....9
6. Scan SAR....9
D. THESIS ORGANIZATION....10

II. IMAGING THEORY FOR MOVING TARGETS....11
A. SCATTERING OF ELECTROMAGNETIC WAVES....11
B. CORRELATION RECEPTION—RADAR DATA MODEL....13
C. RADAR IMAGING—AN INVERSE PROBLEM....15
1. Well-Posed and Ill-Posed Problems....15
2. Data Reconstruction—Regularization....16
D. REFLECTIVITY FUNCTION FOR MOVING TARGETS....16
E. FURTHER SIMPLIFYING APPROXIMATIONS....17
F. IMAGING VIA A FILTERED ADJOINT....18

III. IMAGING ANALYSIS TECHNIQUES....19
A. SYNTHETIC APERTURE IMAGING....19
B. RADON TRANSFORM & FILTERED BACKPROJECTION....21
C. RADAR IMAGING ANALYSIS DEVELOPMENT....22
1. Two-Dimensional Display....23
2. Three-Dimensional Display....24
3. Four-Dimensional Display....25

IV. SYNTHETIC APERTURE RADAR DATA ANALYSIS....29
A. PREDICTION FUNCTION....29
B. TEST DATA DEVELOPMENT....30
1. Velocity Components....30
2. Waveform Comparison....30
C. GRAPHICAL USER INTERFACE DEVELOPMENT....32
D. ACTUAL DATA ANALYSIS....35

V. RESULTS AND CONCLUSION....39
A. IMAGING RESULTS FOR TEST DATA....39

1. Target Imaging in Velocity Space 39
B. IMAGING RESULTS FOR REAL DATA 43
1. Target Imaging in Velocity Space 43
C. FUTURE WORK 44
D. CONCLUSION 44
APPENDIX 47
A. MATLAB CODE FOR PERFECTLY CONDUCTING SPHERE 47
B. MATLAB CODE FOR POINT TARGET ANALYSIS 47
C. MATLAB CODE FOR IMAGE ANALYSIS OF MOVING TARGETS 48
LIST OF REFERENCES 57
INITIAL DISTRIBUTION LIST 59

LIST OF FIGURES

Figure 1. Strip Map mode of SAR Imaging Radar Path From [2] 4
Figure 2. Depression Angle of the Radar System From [1] 7
Figure 3. Azimuthal range diagram From [2] 8
Figure 4. Stripmap SAR Mode From [2] 9
Figure 5. Spotlight SAR Mode From [2] 9
Figure 6. Scan SAR Mode From [2] 10
Figure 7. Radar Cross Section of a perfectly conductive sphere 12
Figure 8. Example of a range profile from a B-727 jetliner. The top view (with orientation at time of measurement) is displayed beneath From [1] 19
Figure 9. Single Pulse imaging of three targets to determine range profile From [1] 20
Figure 10. Multi Pulse imaging of three targets to determine range profile From [1] 21
Figure 11. Scattering geometry From [1] 21
Figure 12. 2-D display of point target at 75 meters,0 meters moving to the right. 24
Figure 13. 3-D display of target correlation horizontal and rotated. 25
Figure 14. 4-D Volume display of target at position 50 meters,0 meters with a velocity of 10 m/s,10m/s. 26
Figure 15. Velocity Terms Used for Analysis 30
Figure 16. Rectangular Pulse in the Time Domain and Frequency Domain From [5] 31
Figure 17. Chirp Pulse in Time Domain and Frequency Domain From [5] 31
Figure 18. Transmitter/Receiver Arrangements Used in Analysis 32
Figure 19. Screen Shot of GUI with Chirp Pulse and Three Point Targets 33
Figure 20. Screen Shot of GUI with Chirp Pulse and Three Point Targets 33
Figure 21. Test cases of two-dimensional point target analysis 34
Figure 22. SIR-C HH data showing large urban area 36
Figure 23. SIR-C data with color enhancement of Oahu 37
Figure 24. SIR-C ENVI processed image showing runway at MCBH Kaneohe Bay 37
Figure 25. Evaluated Imaging System Parameter Table of Variables 39
Figure 26. Chirp Pulse, Four Corner Transmitters/Receivers with 1 Target moving at a velocity (-10,0). 40
Figure 27. Chirp Pulse, Linear Array 8 Transmitters/ 21 Receivers with 1 Target moving at a velocity (-10,0). 40
Figure 28. Chirp Pulse, U Shaped Array 4 Tr/ 4 Rec with 1 Target moving at a velocity (-10,0). 41
Figure 29. Rect Pulse, Four Corner Transmitters/Receivers with 1 Target moving at a velocity (-10,0). 41
Figure 30. Rect Pulse, Linear Array 8 Transmitters/ 21 Receivers with 1 Target moving at a velocity (-10,0). 42
Figure 31. Rect Pulse, U-Shaped Array 4 Txs/ 4 Receivers with 1 Target moving at a velocity (-10,0). 42
Figure 32. IFFT of data set from Backhoe collection. Data provided by DARPA. 43
Figure 33. Correlation plot of target at (0,0) Velocity and Position(0,0) 44

THIS PAGE INTENTIONALLY LEFT BLANK

ACKNOWLEDGMENTS

The author is grateful to his thesis advisor, Professor Brett Borden.

THIS PAGE INTENTIONALLY LEFT BLANK

I. INTRODUCTION

A. RADAR IMAGING

Sensor systems that can detect, locate and identify targets at great distances and in all weather conditions have well-recognized utility. Unlike many other remote sensing systems, radar based systems are known to be capable of performing some of the above described functions over long-range, all-weather day or night conditions unlike many other remote sensing systems. These capabilities stem from to the wavelength of radar signals which makes the signal relatively unaffected by atmospheric and weather-induced attenuation. Herein also lies a problem, since image resolution depends upon signal wavelength [1]. The resultant side effect is that resolution suffers and radar-based imaging will be fundamentally less effective in comparison to other systems based upon relatively shorter signal wavelengths. Nevertheless, radar waves scatter strongly from objects whose size is of the same order as the wavelength. Radar is sensitive to objects whose length scales range from centimeters to meters, and many objects of interest are in this range [2].

Much research and development effort has been expended to improve the use of radar for imaging. It has been reported that resolution on the order of centimeters can be achieved with spotlight mode operation. While the developed techniques have been instrumental in making radar imaging a more viable application, the simultaneous improvements in digital computing have enabled practical systems to be fielded. This has generated great activity in areas such as interferometric synthetic aperture radar (in SAR) and bistatic/multistatic SAR, due to interest in operational concepts [3]. The key to success in all of these applications is the ability to produce high-quality, artifact-free imagery.

With the technology leap in computational capabilities as well as improved civilian SAR systems, a new emphasis has been placed on civilian radar remote sensing. Consequently, SAR has become a common measurement tool, and more attention is being paid to data quality and calibration. SAR systems are being used in airborne and

space-borne applications. The civilian sector has focused on radiometric accuracy and the investigation of natural targets. Meanwhile, military systems priorities have been on detection and recognition of man-made targets (primarily vehicles) against a clutter background [3].

Much work has gone into SAR system development for the acquisition of high quality SAR data, while comparatively little has been developed for the best use of the data acquired. There are two ways that the SAR data can be processed fully exploited to maximize the intelligence gathered from acquired data. One is to investigate the data, its physical content, through experimentation and modeling. The other is to examine the properties that allow the data to mimic real targets. This thesis will concentrate on the former and look to develop a model for moving targets that can be used in the image formation.

1. Radar Basics

The basics of radar, or echo target location, still remain a fundamental component of all radar imaging systems. The issues and tradeoffs that must be made in the design of a radar system are numerous and outside of the scope of this thesis. Radar data is used for target detection and imaging. This radar data is comprised of the received waveform and can be represented as complex valued solutions to the wave equation [1]. The radar system will use a time-varying signal $s_{trans}(t)$ to excite currents on an antenna that launches an electromagnetic wave toward the target. A reflection occurs at the target or other objects and returns to the antenna. The antenna currents are measured and the radar receiver collects a time-varying voltage $s_{rec}(t)$ [1]. Signal processing of the measured data is the main challenge in radar processing: determining information about the target of interest within the $s_{rec}(t)$ data.

The factors determined by power density of the reflected waveform can be estimated by the radar equation in the range of the target and the power density of the transmitted waveform. The radar equation is as follows

Power Density of Reflected Waveform (P_r) = $\frac{P_T g}{4\pi R^2} \times \frac{\sigma}{4\pi R^2} \times A_{eff}$, (1.1)

where P_T is the power density of the transmitted waveform, g is the gain of the antenna, σ is the radar cross section and A_{eff} is the area of the receiving antenna. This equation will serve as a starting point for the development of the radar data that will be used by the signal processor in a radar system. In addition, the target is a single point scatterer in the far field for the majority of this work until tests of the imaging algorithms with real data have been developed to produce images from the collected radar systems.

2. Radar Measurables

Radar systems determine information about the target by various means; range estimation, velocity estimation and bearing estimation. Range estimation is accomplished by measuring the time delay between the transmitted waveform and the reception of the reflected waveform. When multiple radar pulses are used, there can be confusion in matching the echo pulse with the transmitted pulse. The maximum unambiguous range for multiple targets is then:

$$R_{max} = \frac{c + v}{2f_{prf}}, \quad (1.2)$$

where c denotes speed of light, v is the radial velocity of the target and f_{prf} represents the pulse repetition frequency.

Differences in range estimates from pulse to pulse provide velocity estimation. Alternatively, the Doppler frequency shift gives the radial velocity

$$\omega' = \sqrt{\frac{1 + v/c}{1 - v/c}}\omega, \quad (1.3)$$

when v<<c. This can becomes approximately: $\partial\omega = \omega' - \omega = kv$ where $k = \omega / c$. The target and radar introduce Doppler shifts in the transmitted waveform, up or down depending on relative speed. The round trip Doppler shift is $2kv$ and by dividing by $2k$ gives the radial velocity of the target.

Bearing estimation is accomplished by one of two methods. Using a narrow beam, high directional gain antenna and maximizing the return of the target, provides bearing. To improve the bearing precision, requires using a monopulse radar system. This involves either phase comparison or amplitude comparison of the monopulse signal can be done by sampling the wave front at different locations and estimating its normal direction [1].

B. SYNTHETIC APERTURE RADAR

1. System Parameters

Synthetic aperture radar, SAR, is a coherent imaging approach that overcomes the short comings of real-aperture radars. The concept is to create a long synthetic aperture by moving a small antenna along the path of the platform flight path(or orbit) and then properly processing the received signals,[4] Figure 1 coherently, shows the profile for a SAR platform and sensor scanning in strip map mode.

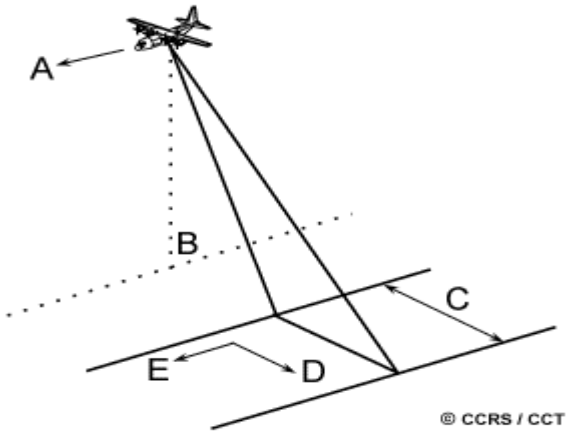

Figure 1. Strip Map mode of SAR Imaging Radar Path From [2]

The aircraft in the figure, is traveling with a velocity in the A direction over the point B on the ground, carrying a side looking radar antenna. The direction of travel defines the “azimuth” direction E and the distance from B to the imaging area on the ground is the range direction, D. The actual swath, C, depends on mode of operation and the actual antenna size, wavelength and the geometry of the aircraft and target area. The typical SAR antenna is of rectangular shape and is measured with dimensions in azimuth

and elevation. The radiation spreads out from the antenna in a pattern determined by its length. This angular spreading (or "beamwidth") is $BW = \lambda / d$, in radians, where λ is the wavelength of the wave transmitted by the radar and d is the length of antenna along that dimension[2]. The beamwidth becomes the fixture for the different modes of operation and Chapter II considers these effects.

2. Data Sampling

Both data acquisition and signal processing by SAR sensors are becoming more and more demanding with the increasing capabilities of sensors as well as power sources. Remote piloted aerial vehicles as well as space based platforms demonstrate the utility of SAR systems. Digitizing the analog signal and storing the result in computer memory provides a finite-length, data-array needed for subsequent processing. The system designer can select the bandwidth of the radar signal and the size of the target area for the range contribution. This ties back to the classic problem of representing an analog time or spatial domain signal via a finite sequence, its Fourier transform via another finite sequence, and the tolerable aliasing errors, which are unavoidable [5].

The first of the choices is radar bandwidth. The transmitted radar echo has energy within a finite band in the frequency domain (i.e., it is bandlimited). The echo signal s(t) is a linear combination of shifted versions of the transmitted radar signal p(t). To avoid aliasing the echo signal s(t), the sample rate must satisfy the Nyquist sampling criterion and range resolution:

$$\Delta t \le \pi / \omega_0 ; \Delta x = \frac{c}{2} \Delta t_{\max} = \frac{c\pi}{2\omega_0} \quad [3].$$

The next choice for the system designer is the target support area or the sampling time interval choice. A center point at range R, determines the target area by adding and subtracting an equivalent distance X_0 to or from the center point. The closest target reflection in the scene will arrive at the receiver at some time T while the farthest reflectoion in the scene will arrive at the receiver at some time T + ΔT. The system will have to acquire time samples of the echoed signal s(t) over this time interval to capture the echoed signals from all the reflectors in the scene.

C. SAR IMAGING

1. Resolution

The concept of resolution comes from earlier work with optical systems with a consistent theoretical framework. Radar resolution introduces its own terms and meanings for each of the two resolution directions; range, (across-track) or azimuth, (along-track). Radar resolution is the minimum separation between two objects of equal reflectivity that will enable them to appear individually in a processed radar image [4]. The radar community uses the terminology, the "impulse-response" function to define resolution. The purpose of a radar system is to distinguish individual targets; the impulse-response function defines the ability of the system to distinguish single point targets. Radar resolution is quirky in that resolution in range and azimuth derive from different physical processes, and tend not to be the same because antenna sizes in these two dimensions are different.

2. Radar Range Resolution for SAR

The minimum spacing between two objects that can be individually detected defines radar range resolution. To expand on that definition: in order for a radar system to discern two targets in the range, or across-track dimension, all parts of their reflected signals must be received at the antenna at different times [4]. In order to define range resolution, the slant range depends on the range of pulse transmission intervals to the targets. The slant-range resolution measured in the across-track dimension in equal to one-half the transmitted pulse. Ground-range resolution R_{gr} depends on the β depression angle of the sensor, as:

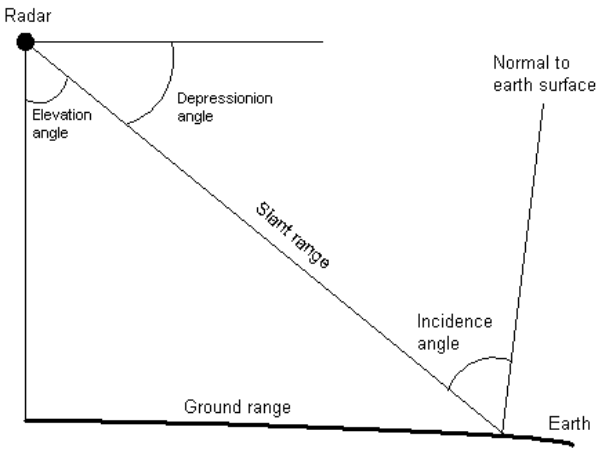

Figure 2. Depression Angle of the Radar System From [1]

$$Slant\ range = \frac{c\tau}{2}\ or\ Ground\ range = \frac{c\tau}{2\cos(Depression\ angle)} \quad . \quad (1.4)$$

Decreasing the depression angle or increasing range will maximize ground resolution. Across-track resolution is better in the far range than in the near range will maximize the ground resolution by Shortening the pulse length will improve the resolution but there are limitations in reducing the pulse length too much and thus not having sufficient energy for the echoes of the wave to be detected by the receiver. Increasing power will offset the energy decrease at the receiver but a higher peak power is required. A pulse length of a few microseconds will give a range resolution of some hundreds of meters.

Simply reducing the pulse width in an effort to improve the range resolution is not practical because the high peak power is difficult to accomplish. One method to overcome this limitation and improve range resolution is pulse compression. Pulse compression replaces the short pulses by long modulated pulses, provided that they are followed by a processing step. A typical modulated long-pulse waveform, is the 'FM chirp' pulse. The FM chirp pulse has frequency that increases linearly with time. The benefits of the FM chirp is that illuminated objects that have different frequencies of the returns, even if they overlap in the time domain. The inverse relationship of the FM chirp to pulse width provides range and spatial resolution due to an. The chirp can be much

larger than the inverse of the pulse-width. An example is that of the SIR-C X-Band system—transmitted a 9.61 GHz signal with a 9.5 MHz chirp bandwidth. This system in low earth orbit had a 15 meter range resolution [4].

3. Radar Azimuthal Resolution for SAR

The real beam radar azimuthal resolution, otherwise known as the along-track resolution, is determined by the width of the ground strip that is illuminated by the radar system. Two targets at the same range can only be separated if they are not within the same radar beam at the same time. The size of the radar beam is determined by the physical dimensions of the radar antenna. Azimuthal resolution can be improved by reducing the wavelength of the carrier frequency and/or increasing the antenna dimensions so that beamwidth is reduced [6]. Neither of these methods are very practical in a physical sense, but the antenna dimension can be increased synthetically. The method used for creating a synthetic aperture of a large antenna along the path of motion combines the received echoes coherently along the flight path overcomes the limitations of the real beam radar. A radar system with an antenna length, L, will have a main beam footprint on the surface with characteristic length of $2\lambda/L$. A sequence of pulses will illuminate a target for as long as the along-track velocity keeps the beam on the target.

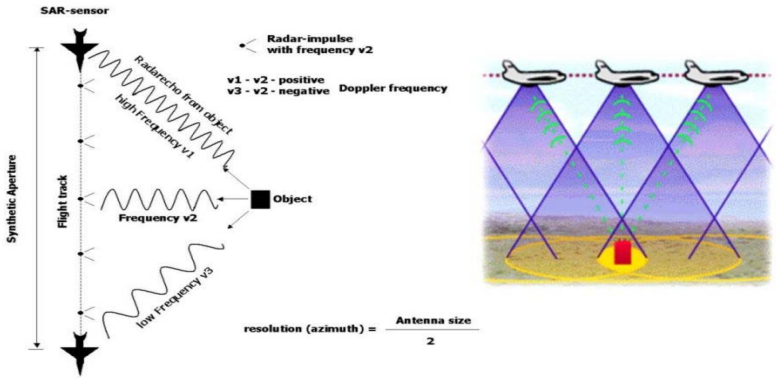

Figure 3. Azimuthal range diagram From [2]

4. Stripmap SAR

Stripmap is the most popular and generally used mode of SAR imaging. The radar antenna points in a fixed direction along one side of the path of the radar platform,

whether it is airborne or spaceborne. The antenna pattern covers a path that illuminates a strip on the surface as the platform moves. The strip-map mode, the across-track (range) resolution is less than the along track (azimuth) direction. The high azimuth resolution (typically 10m) comes from integrating successive echoes from a given target over the time interval that illuminates the target. The effective azimuth aperture of the synthetic antenna is up to several kilometers [4].

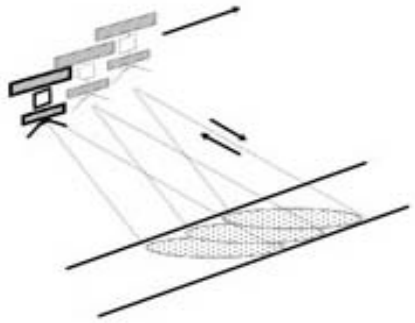

Figure 4. Stripmap SAR Mode From [2]

5. Spotlight SAR

In addition to stripmap mode, spotlight mode operation will increase the resolution. The radar antenna points to a specific target region for the entire data collection sequence. This mode gives increased azimuth resolution at the cost of decreased coverage.

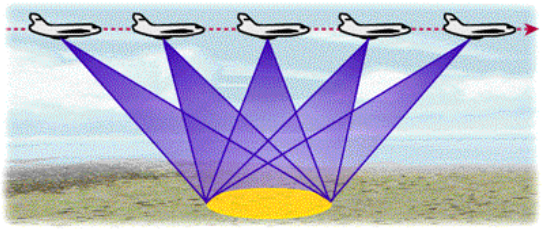

Figure 5. Spotlight SAR Mode From [2]

6. Scan SAR

A third option for SAR operation maximizes the benefits of the previously mentioned modes. Scan mode allows for a dramatic increase in coverage area by periodically stepping the antenna beam to adjacent antenna footprints in the range direction [6]. The synthetic aperture length of each sub-swath determines the resolution.

This decrease in synthetic aperture length will decrease the azimuth resolution with respect to stripmap mode. The bottom line is that as swath coverage in the range increases, the azimuth resolution decreases.

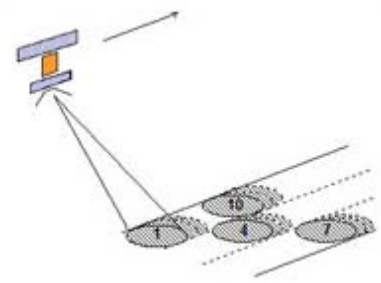

Figure 6. Scan SAR Mode From [2]

D. THESIS ORGANIZATION

This thesis will attempt to show the improvements on the algorithms developed for the imaging of moving targets within a data scene utilizing synthetic aperture radars. Codes for image analysis were developed as well as codes to read different data sets from a variety of sources. The first task was to leverage unclassified data sets and show the capabilities of the developed imaging codes. The second task, at the successful completion of the first, was to apply the reader codes and imaging codes to classified data sets to show actual improvements in the imaging of moving targets. This work did not develop a user interface for the data analysis, but merely a capability to analyze the data and make determinations of the moving target image techniques being applied. An important task was to develop methods for displaying four-dimensional radar data.

II. IMAGING THEORY FOR MOVING TARGETS

A. SCATTERING OF ELECTROMAGNETIC WAVES

Thus far, the basics of radar operation have been discussed as well as the modes of operation for a Synthetic Aperture Radar system. In order to properly analyze the imaging theory for moving targets, an understanding of the radiated energy from the radar, the scattering of electromagnetic wave as well as its reception of the reflected energy is required [1].

An electromagnetic wave can be completely described by Maxwell's equations

$$\nabla \bullet D = \rho \tag{2.1}$$

$$\nabla \bullet B = 0 \tag{2.2}$$

$$\nabla \times \mathbf{E} = -\frac{\partial \mathbf{B}}{\partial t} \tag{2.3}$$

$$\nabla \times \mathbf{H} = J + \frac{\partial \mathbf{D}}{\partial t} \tag{2.4}$$

Together with the Lorentz force law

$$F = q(E + v + B) \tag{2.5}$$

these equations are the fundamental equations needed for the understanding of electromagnetism and allow for the description of any time-varying disturbance of the electric and magnetic field [1]. The far field approximation implies that the target is very far from the source and is a commonly used approximation applied to Maxwell's equations. A key component of the far field approximation is that the incident wave approximates a plane at the target; consequently the wave has no dependence on coordinates perpendicular to the direction of travel of the wave. A harmonic wave emanating from of a finite sized object in the far field is of the form

$$W(r, k) = \frac{e^{ikr}}{4\pi r} F(\theta, \varphi), \tag{2.6}$$

where $F(\theta, \varphi)$ is the far-field pattern associated with the finite object [1].

Understanding radar scattering requires an appreciation of the complexities of the wave, its properties and its interaction with targets. Scattering from a perfectly electrical conductive surface is complicated to model and define even when the boundary conditions are simple. Generally, radar applications utilize an incident wave at the low frequencies that are utilized for radar applications, will create evanescent waves that penetrate to a skin depth. These waves will induce a current as well as interfere. A wave incident upon a conductive surface will accelerate charges in the conductor. For a simple case of a perfectly conducting target, the charges have no resistance to motion and respond immediately to the incident field. The moving charges become a current distribution that creates radiation in the form of a scattered field. The overall field, incident and scattered must satisfy Maxwell's equations [1].

Figure 7 shows the characteristic behavior of the fractional back-scattered energy as a function of wavelength. The plot represents the reflected energy for a plane wave incident on a perfectly conductive sphere.

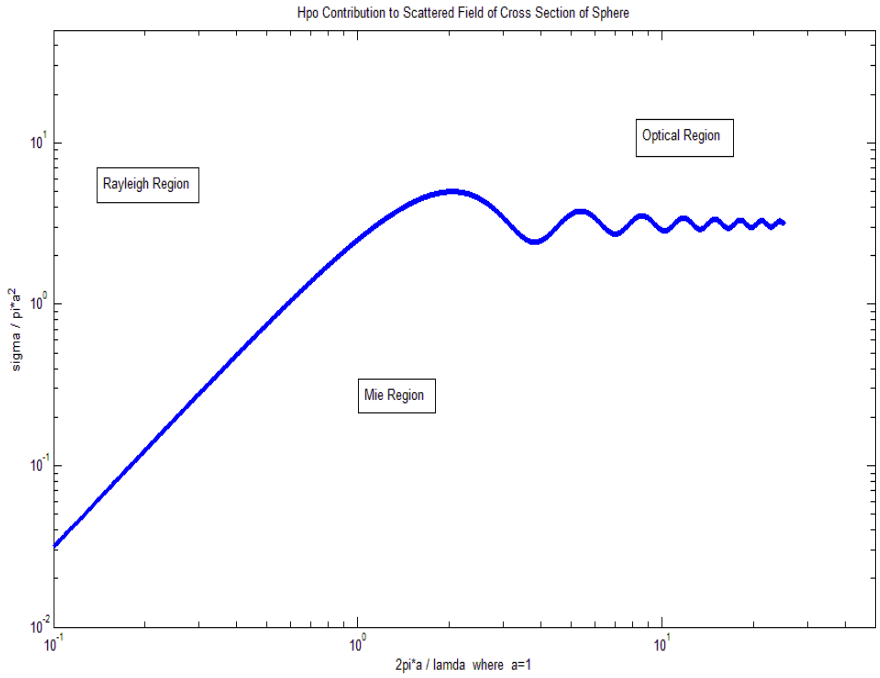

Figure 7. Radar Cross Section of a perfectly conductive sphere

In Figure 7, the Rayleigh region to the left represents where the sphere circumference is much smaller than the wavelength and the scattered energy is proportional to the fourth power of the frequency. In the Mie region, the sphere and the wavelength are of the same order of magnitude giving rise to resonances as the wave and electrons travel around the sphere producing both constructive and destructive interference. In the optical region, the object is much larger than the wavelength and it is valid to consider the incident wave as geometric rays bouncing off the surface. The back scatter cross section of the target in the optical region is approximately the projected area of the target $\approx \pi a^2$.

Another method to model the scattering, when the boundary conditions at the surface of the scatterer do not coincide with the coordinate system, is the integral equation approach. With the improvements in digital computing capabilities, this method has become the basis for the modern radar scattering prediction methods.

The development of a scattering model is critical for our understanding of the radar data that is created. The proven approach of using the scattering center description of the target describes $H_{scattered}(\mathbf{R},t,k)$ in terms of the generalized scatterer density function $\rho_{k,\mathbf{R}}(x)$ [1]. An ideal radar system will actually transmit a vector-valued incident pulse $H_{inc}(x,t)$ and the measure (components of) a vector-valued echo $H_{scattered}(x,t)$ reflected from the target. The usefulness of this approach allows for the development of the weak-scatterer far-field model that leverages both the physical optics and geometric optics. When applying conditions to the target and defining the coordinate system in terms of cross range and down range, the "standard" target model; or weak, far-field model is:

$$H_{scatt}(R,t,k) = \frac{H_0 e^{i(2kR-\omega t)}}{4\pi R}\int \rho_{k,R}(x')e^{i2k(y'\cos\theta - x'\sin\theta)}d^3x' \qquad (2.7)$$

where $x' = x'\hat{i} + y'\hat{j} + z'\hat{k}$ and θ is the aspect angle, (see Figure 10).

B. CORRELATION RECEPTION—RADAR DATA MODEL

The correlation receiver allows the radar to detect targets at great distances. The radiation of a wave from an antenna and the reflection of that wave off a target both fall

off as the inverse square of the distance traveled. That produces a decrease in signal strength proportional to the inverse of the distance, R^4. This is the principle driver in that limits the detection ranges of targets. Increasing the power and pulse integration will help but these techniques can not usually overcome the R^{-4} drop in power that occurs [1]. Other factors limit maximum range as well; the maximum unambiguous range increases inversely as the pulse repetition frequency, and the movement of the target during data collection will alter the phase of the scattered field [1]. The correlation receiver is elegant in that it provides an optimal separation of a meaningful signal from the unwanted noise background.

The theory of the correlation receiver is based on its ability to separate the scattered signal of the target from the random, incoherent noise in the system. The scattered signal is comprised of the range and range-rate. The signal time-delay and frequency-shift of the scattered wave determine these values. The received signal consists of the scattered signal and additive noise where the noise is a random process [1]. The goal of a correlation receiver is to separate the scattered signal from the random measurements at the receiver. Scattering of the incident wave upon the target provides the natural model for radar. The incident wave comes for the radar and the scattering model involves superposition of the target reflectivity density and a signal offset that is proportional to the time delay and range of the target and Doppler shift from target motion. The correlation receiver is looking for a portion of the received signal that is similar to a time-delayed and frequency shifted version of the transmitted signal. The portions of the received signal that do not look like the transmitted signal such as noise will correlate to zero [1]. The standard radar data model that expresses the output $\eta(\nu,\tau)$ of the correlation receiver is

$$\eta(\nu,\tau) = \iint \rho(\nu',\tau')\chi(\nu-\nu',\tau-\tau')e^{i\frac{1}{2}((\nu-\nu')(\tau-\tau'))}d\tau' d\nu' \cos^{-1}\theta, \qquad (2.8)$$

where τ is the range variable, ν is the range rate variable, ρ is the target reflectivity density and χ is the radar ambiguity function [1].

C. RADAR IMAGING—AN INVERSE PROBLEM

A liner, shift-invariant system approximates a radar imaging system well. This proves to be valuable as it states that the input object function *f(x)* at each point *x* has a corresponding output image *m(x)* formed by simple superposition. The imaging system measures targets with the same input and output functions regardless of when they start or where they are located. Radar imaging will not be meaningful if the delayed version of the target looks different from a simple shift. In other words, if a different images appear with each successive pulse of the imaging system, that will not be a useful image. A method of understanding and comprehending this imaging problem is to consider an imaging system represented by the functional operator ("kernel") κ that describes how the imaging system measures the object function

$$m = \kappa(x). \qquad (2.9)$$

The problem for the imaging system is the mapping from target to system mapping coordinates measured by the imaging system. This problem is known as an *inverse problem*, that focuses on reproducing the original target from the given data and knowledge of the imaging system measurements and scattering model.

1. Well-Posed and Ill-Posed Problems

The inverse problem is complicated by the ill-posed nature of the solution in that the solution is not unique. The solution may not exist for particular set of measurement data or the solution does not depend continuously on the measurement data. The band-limited nature of imaging systems only adds to the ill-posed problems in that the imaging system does not measure information about the target outside the band of the imaging system. The ill-posed nature of the imaging system can be represented as

$$f = \kappa^{-1} m, \qquad (2.10)$$

where κ is an ill-conditioned matrix and f is the object function.

The imaging system kernel κ imposes properties on the measurements. The matrix κ has a size of is N x M $(M > N)$ as the object function of possibly infinite

dimension. The imaging system has band-limited limitations, for its dimensionality. There are more unknowns than there are linearly independent solutions, so the imaging system cannot have a unique solution.

The object data space is M-dimensional and typically larger than the measurement space (N-dimensional). It includes a null space, which contains all data that cannot be measured. The kernel κ in the null space is determined by and accounts for measurement errors and artifacts. In an attempt to solve for this sparse infinite data set, a common and accepted method is to search for approximate solutions that satisfy additional physical constraints. The set of approximate solutions corresponding to the same kernel κ is the set of objects with images close to the measured one and expressed by the following normal equation

$$\kappa^T \kappa f = \kappa^T m, \qquad (2.11)$$

which is, in many cases, equivalent to a least squares solution.

2. Data Reconstruction—Regularization

The physical conditions that constrain the ill-posed problems solution must satisfy a least squares solution for *f*. The measured data suffers from finite dimensionality and imaging system artifacts. This develops into a bigger problem because the kernel κ is poorly conditioned and the imaging system artifacts, noise, are magnified as the dimensionality of the imaging data set gets larger. There are two methods used to mitigate the effects of imaging system artifacts when estimating *f*. They are the truncated singular value decomposition and Tikhonov regularization [1].

D. REFLECTIVITY FUNCTION FOR MOVING TARGETS

The general SAR imaging system cannot resolve the relative position of a target when it moves with an unknown velocity. Without a priori knowledge of the target's relative orientation, artifacts will be created. The most notable visualization of this artifact is that of the 'train off the tracks.' Imaging of moving targets requires a more general algorithm.

The scattering behavior of the target describes the reflectivity function $\rho(x)$ is completely described. This function represents a scale factor of the received signal strength and a critical piece for the imaging system [1]. In the case of a moving target, the reflectivity function will become a time-varying function $\rho(x,t)$. The basic principle behind imaging moving targets is the wave emanating from the imaging system at time t. The wave interacts with a target at time t'. During the interval of time t to time t', the target moved from x to $x+vt'$. The wave scatters off the target with strength $\rho_v(x)$ and then propagates from position $x+vt'$ to position z arriving at time t. The reflectivity of all targets moving with different velocities v, with a scatterer density at time t and position x will become the reflectivity function.

$$\rho(x,t) = \int \rho_v(x - vt) d^3v \qquad (2.12)$$

E. FURTHER SIMPLIFYING APPROXIMATIONS

The scattered wave function from a moving target, described above using the reflectivity function of moving targets, applies to very general circumstances. The function is a manifestation of retarded-time problems, which are invariably complex [1]. Complications arise for retarded-time obtained implicitly. A more tractable result occurs when the scatters are moving with a known velocity vector, with a Taylor series expansion of the vector around t = 0 and the scatter is "slow moving."

The slow-mover, narrow-band and far-field approximation will minimize the complexity of the ill-posed problem for the imaging system. The slow mover approximation is when ($|v|t$) is much less than $|x-z|$, where x denotes the position of the target and z denotes the movement of the target for the velocity component in the target-transmitter direction [1]. The narrow band approximation is determined when transmitted signal is slowly varying in comparison with the carrier frequency. Far-Field approximations is valid when the transmitter-to-target and target-to-receiver distances are large in comparison with the scene dimensions [1].

F. IMAGING VIA A FILTERED ADJOINT

The imaging system leverages the correlation receiver's technique of cross correlation to compare and project how much a function looks like another function. The "best fit" of the data to the scattering model will represent how well the correlation matches [1]. The previous sections detailed the scattered field and its measurement within the receiver and the method for determining the model for data of our imaging system.

This correlation between the model and data depends upon the target position in three-dimensional space and the velocity vector. The scattering model for the imaging system uses these six parameters. The maximum cross correlation of the six-dimensional model data and the scattered signal received by the imaging system will localize the position and velocity of the unknown scatterers in phase space (position-velocity space) [1]. The term, "imaging" refers to localizing the cross correlation in two dimensions and this technique can generate hyper images that combine multiple position and velocity dimensions [1].

An imaging system using this cross correlation approach does not depend on knowledge of exact position of the target, since any time shift will translate to our image in range only. The band-limited cases of the imaging system will not actually perform a true cross correlation; the image of the system will be a "practical, best approximation" to the cross correlation.

III. IMAGING ANALYSIS TECHNIQUES

A. SYNTHETIC APERTURE IMAGING

With the development of filtered adjoint imaging, now the emphasis shifts to a "target interpretation" problem. One-dimensional imaging involves the generation of range profiles, which can articulate target substructure. For high range resolution (HRR) techniques, the imaging system's transmitted pulse, instantaneous, range-resolution is smaller than that of the target. As it sweeps across the target, it sequentially excites the target's scattering subelements, which re-radiate energy back to the imaging system receiver. For non-interacting, point-like, scattering sub-elements, the scattered pulse is a sum of damped and blurred images of the incident pulse, which are shifted by time delays that are proportional to the subelement's range [1]. Figure 8 shows an example of one-dimensional images created by HRR radar systems. The profile displays additional peaks outside of the target and shows evidence of the single, non-interacting scatterer approximation problem.

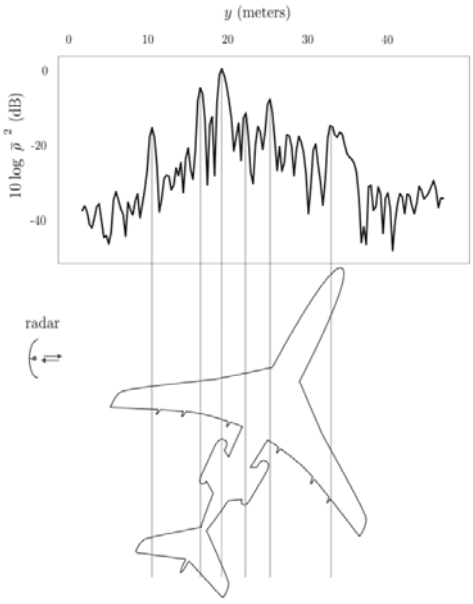

Figure 8. Example of a range profile from a B-727 jetliner. The top view (with orientation at time of measurement) is displayed beneath From [1]

A variety of factors, such as target aspect angle, position of the scatterers or masking of scatterers by other parts of the target, effect the down-range profile.

Additionally, while the use of short pulses enhances the resolution, it simultaneously leads to large bandwidth requirements. A short-pulse waveform also provides less accurate radial velocity measurement, a natural consequence from the properties of the radar ambiguity function. As described in Chapter I, an important limitation for practical radar applications is the higher peak transmitted power for short pulses over long ranges. Radar target recognition using only range profiles has limited application. This is because a range profile will not be able to distinguish cross-range target structures. All scatterers located at the same distance from the radar will reflect energy back to the radar with the same time delay.

An imaging system can leverage a relatively simple idea based on "triangulation" that builds the cross-range target information using an high range resolution technique. The theory behind this technique is to collect the range profile of the target from many different target orientations; then correlate them to each other. This is shown in the following figures for three targets. The first shows that target 2 and target 3 cannot be resolved with a single pulse. The next figure shows that multiple pulse imaging from the imaging system can determine the range profile of the three targets.

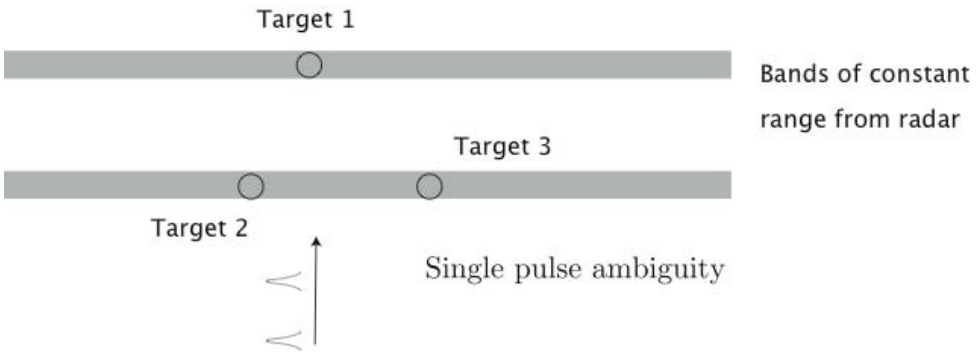

Figure 9. Single Pulse imaging of three targets to determine range profile From [1]

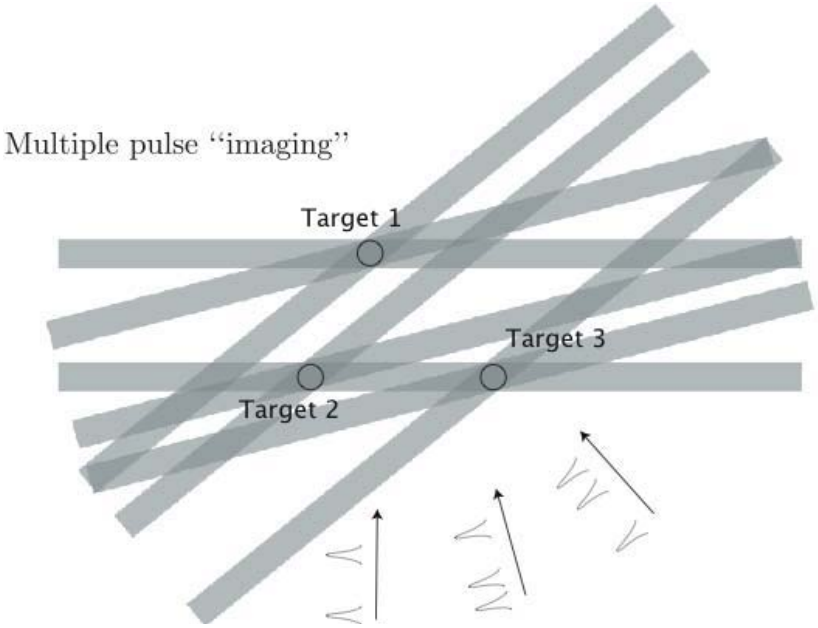

Figure 10. Multi Pulse imaging of three targets to determine range profile From [1]

B. RADON TRANSFORM & FILTERED BACKPROJECTION

Multiple aspects or "looks" at the target will recover the range and cross-range information. The goal of the imaging system is to distinguish the multiple range profiles from each "look" by labeling them with the imaging system target orientation. This is important as the scattering density function discussed previously depends on target orientation.

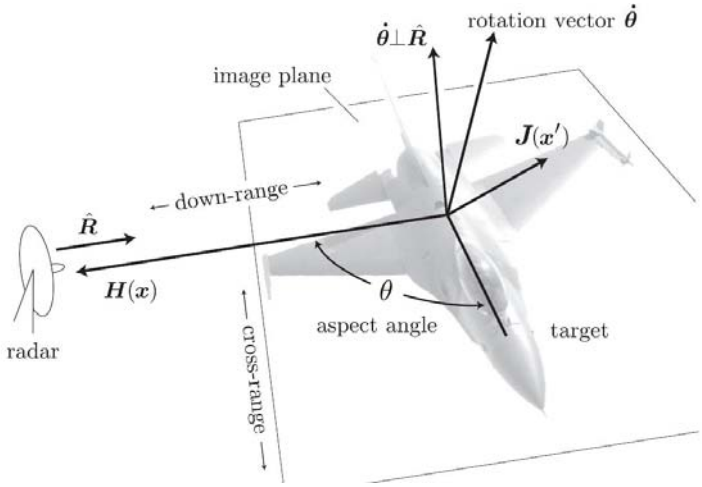

Figure 11. Scattering geometry From [1]

The imaging system will attempt to resolve this complexity by assigning a coordinate system fixed to the target. The scattering density function then becomes a rotated version of the stationary target.

The next step in algorithm development for image processing is to fix the rotation of the target and apply the 2D Fourier transform sampled at the spatial frequencies $\kappa_x = -\omega\sin\theta$ and $\kappa_y = \omega\cos\theta$. Using the Projection Slice theorem the power P is:

$$P(-\omega\sin\theta, \omega\cos\theta) = \int_{-\infty}^{\infty} \rho(\tau) e^{-i\omega\tau} d\tau. \qquad (3.1)$$

An inverse Radon transform by using the backprojection operator and the filtered backprojection algorithm can build up an image [1].

C. RADAR IMAGING ANALYSIS DEVELOPMENT

The SAR imaging system is a complicated device whose purpose is to measure the interaction of an incident wave upon a surface, whether that is an airborne target or the earth's surface, and then produce an image from these that measurements. The ability to turn a three-dimensional set of measurements into usable information is the goal of the imaging system. A basic requirement is that an image tell the user something of interest to them?[2] The information gleaned from the imaging system depends on knowledge of electromagnetic field theory, general world knowledge, and understanding of the user.

One of the most challenging issues for the imaging system regarding the data is that of the inverse problem; what properties of the unknown scene can be determined or estimated from the received backscatter signal. The problem lies in the amount of information provided to the imaging system and rarely is there enough of this information for a unique solution [3]. The inverse problem generally relies on some a priori knowledge for successful solution. Experience shows that the brain attaches high information content to vertices, linear structures, and edges; then "fills in" areas to characterized the image by regions [3].

1. Two-Dimensional Display

A radar display is typically on an X-Y plane that shows a position of the target in relation to the transmitter/receiver. This data can be superimposed on a map for enhanced understanding of the position. The display shows velocities of the target and this is normally accomplished by using an icon attached to the target that shows a calculated velocity and heading of the target. The data from the Phase Space algorithm will estimate a position in three dimensions, as well as a three-dimensional velocity vector and the image that is produced will display that information.

The first approach is to display the data in a two-dimensional display utilizing the Matlab *imagesc* function. The *imagesc* function scales image data to the full range of the current *colormap* and displays the image. A processed data array for the image of the correlation of real data and expected data is a square matrix that is NxN where N is the number of transmitters/receivers for the current configuration. In general, the number of transmitters is different from the number of receivers. The display shows the correlation of a target moving at certain velocity and the expected velocity as a point at the target position. In this scheme, data displayed as a two-dimensional plot with velocity held constant; multiple velocity displays are needed to show multiple velocities of the different targets. The multiple displays are not practical for operational use and other methods to show position and velocity are needed.

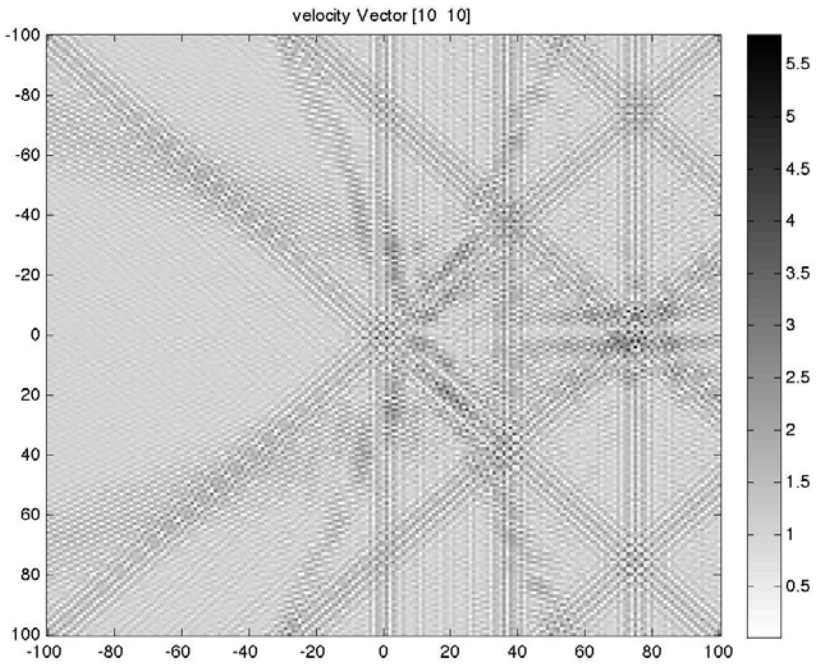

Figure 12. 2-D display of point target at 75 meters,0 meters moving to the right.

Figure 12 shows the two-dimensional display of a single target that starts at position (X,Y) equal to (75,0) meters and moves at a velocity of ten right and ten up (V_x,V_y) equal to (10,10) meters. The display is easy to understand and determine where the target is located. This particular graph shows a small point target but the higher resolution shows the artifacts that are inherent in this transmitter/receiver configuration. This a plot of all targets moving at a velocity (10, 10) meters and thus why this is a useful display of the data for operational purposes but could be improved due to its limitation in velocity plotting. This limitation is imposed by the code selecting all targets moving at the velocity (10,10) meters. The code has been shown to select a range of velocities and plot them, which begins to give more useful information to the operational user.

2. Three-Dimensional Display

Displaying three-dimensional data is easily accomplished in Matlab with results that are intuitive and pleasing to the eye but not very practical for operational purposes. The first decision that must be made is the choice of which three-dimensions will be

mapped to the display. The plot will be displayed using the *mesh* or *surf* functions in Matlab. The *mesh* is drawn as a surface graphics object where the face color is the same as the background color (to simulate a wireframe with hidden-surface elimination), or none when drawing a standard see-through wireframe. The current *colormap* determines the edge color [9]. The *surf* function is similar to the *mesh* function except that it creates a shaded surface plot.

These two functions were systematically adjusted with to determine the optimum choice for display of the data. The X-Y position and the magnitude of the velocity were chosen to be plotted in the three-dimensional display. This approach was appropriate for checking the validity of the code for image analysis but not very functional for the operational user.

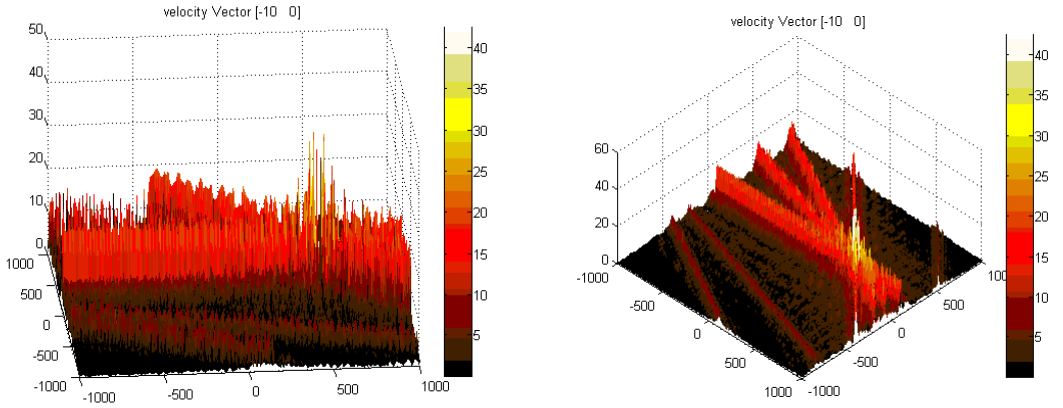

Figure 13. 3-D display of target correlation horizontal and rotated.

Figure 13 shows the display of the correlation of a target that is located right of the axis with a velocity in the left direction. The emphasis is to show that the three-dimensional display is useful to detect a correlation. The plot also shows the artifacts that are inherent in the data. What is not known about the target is its velocity direction.

3. Four-Dimensional Display

Displaying four dimensions becomes a challenge due to the nature of the display method. Matlab functions that display data with four dimensions include the *scatter* and *slice* functions. The *scatter3* routine displays colored circles at the locations specified by

the vectors X, Y, and Z (which must all be the same size). The fourth-dimension input determines the size of each marker (specified in points), this input can be a vector with the same length as X, Y, and Z, or a scalar [9]. The *slice* function displays orthogonal slice planes along the *x, y, and z* directions in the volume V. The volume V is an *m*-by-*n*-by-*p* volume array containing data values at the default location X = 1:n, Y = 1:m, Z = 1:p. Each element in the vectors sx, sy, and sz defines a slice plane in the *x*-, *y*-, or *z*-axis direction [9].

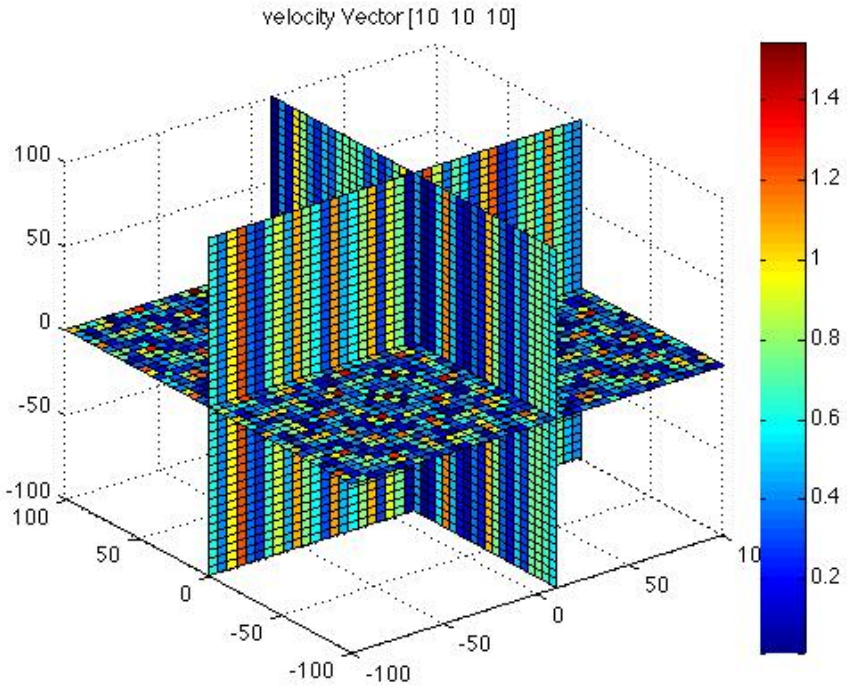

Figure 14. 4-D Volume display of target at position 50 meters,0 meters with a velocity of 10 m/s,10m/s.

Figure 14 is the *slice* display of the correlation of a target that is located right of the axis and having a velocity in the left direction. This plot is not useful without more a priori knowledge of the target. The plot also shows the artifacts that are inherent in the data.

The described plotting methods in Matlab were used to evaluate the prediction function of the Phase Space algorithm. The displays all have attributes that make them

useful but more information can be gained by combining the plots and selecting certain criteria for information that is desired. The next chapter will describe the development of a graphical user interface that will explore various configurations of transmitter/receiver combinations as well as different display tools for the processed data.

THIS PAGE INTENTIONALLY LEFT BLANK

IV. SYNTHETIC APERTURE RADAR DATA ANALYSIS

A. PREDICTION FUNCTION

The Phase Space algorithm developed by Cheney/Borden accounts for both velocity and position while imaging the target. The principal element enabling this capability is the prediction function. The prediction function is the model of the expected data collected by the radar imaging system for a known target (position and velocity). This function will be correlated to the measured data to form an image. The prediction function has the form.

$$\Psi_{SCAT}(t) = \int s\left(\alpha\left(t - \frac{R}{C}\right) - \frac{R}{C}\right) q(r,v)\, dxdydzdv_x dv_y dv_z \tag{4.1}$$

where he first term in the integrand, s, is defined by the waveform used by the imaging system. This term describes the type of pulse that the radar system is utilizing to image the target. The various waveforms will be described later as an input to the graphical user interface for analysis of various imaging system parameters. The argument of the function, *s*, is

$$\left(\alpha\left(t - \frac{R}{C}\right) - \frac{R}{C}\right) \tag{4.2}$$

which defines the Doppler scaling and range shifting factor. When the target is stationary, α=1, and the argument of *s* reduces to the familiar

$$\left(t - \frac{2R}{C}\right). \tag{4.3}$$

The second term of the integrand represents a target at position r, with velocity v, with strength of q. The prediction function is integrated over all positions x, y, and z as well as all velocities with components in directions x, y, and z to yield the fully multistatic scattered field model.

B. TEST DATA DEVELOPMENT

The development of the Phase Space algorithm is shown that the multi-dimensional point spread function will accurately localize a point target's velocity and position components. This development has progressed so that those same synthetic point targets used for the point spread function analysis is imaged using an imaging process. Imaging of these point targets displays the target's position as a function of velocity or the target's velocity as a function of position.

1. Velocity Components

The Phase Space Algorithm developed by Cheney/Borden is capable of determining the velocity of a target based on time or frequency domain measurements made by the radar imaging system of the reflected wave and comparing then to the model that accounts for the velocity components. The code developed for the imaging of the point targets can account for various velocities of targets, from stationary to extremely fast velocities. These velocity components have been tested and demonstrated to be correctly displayed utilizing the Cheney/Borden algorithm. The test protocol, as shown in (Figure 15), and results will be discussed in the following sections as part of the Graphical User Interface discussion.

V_X – Direction	V_Y – Direction
-10	-10
-5	-5
0	0
5	5
10	10

Figure 15. Velocity Terms Used for Analysis

2. Waveform Comparison

In addition to the velocity components of the target as adjustable variables in the prediction function, the source waveform is adjusted. The source waveform varies as

needed by the radar imaging system's desired output product. The source terms utilized for this project were rectangular (*rect*) functions(Figure 16), chirp functions and chirp step functions.

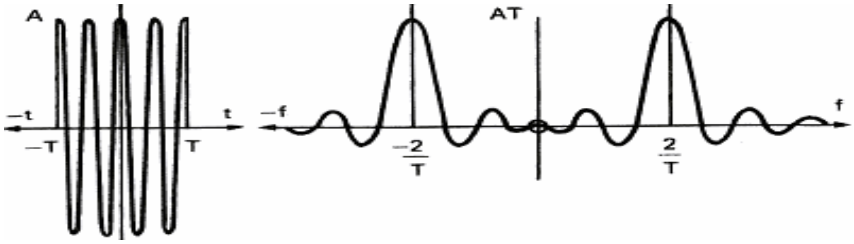

Figure 16. Rectangular Pulse in the Time Domain and Frequency Domain From [5]

Chirp pulses or Linear frequency modulated (LFM) pulses are often used in sonar and radar applications. The LFM pulse, is defined below and in shown in Figure 17:

$$s(t) = A\cos\left(\Omega_0 t + \frac{\pi W}{T}t^2\right) \qquad -\frac{T}{2} \le t \le +\frac{T}{2} \qquad (4.3)$$

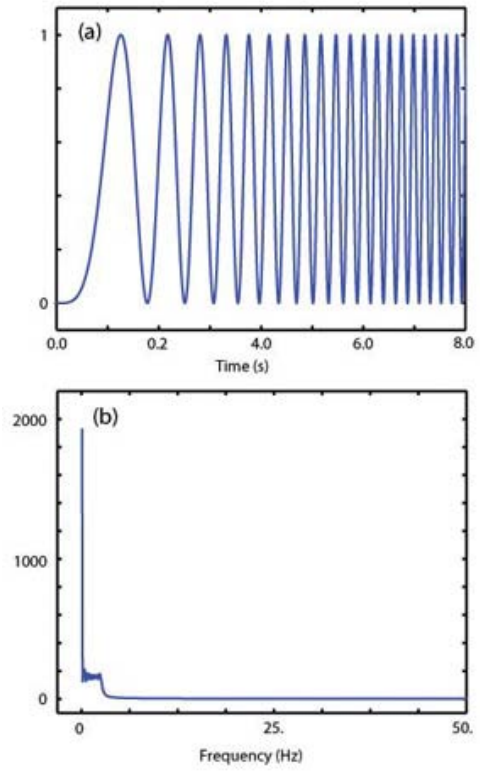

Figure 17. Chirp Pulse in Time Domain and Frequency Domain From [5]

C. GRAPHICAL USER INTERFACE DEVELOPMENT

The development of a systematic method to determine optimum imaging system performance is the objective of the graphical user interface(GUI). The design of the GUI is based on a capability to determine what source waveform and transmitter/receiver combination will yield optimum results for the imaging system. As inputs to the GUI, the waveform is first selected. As previously discussed, the types of input waveforms examined were rectangular, chirp and step-chirp functions. These waveforms were selected due to their use in most radar imaging systems. The analysis must include various waveforms to determine the best source term for a variety of velocities from slow to fast.

In addition to the waveform, another factor for determining radar imaging system performance is the physical arrangement of the transmitters and receivers. This can be the position of fixed systems or the flight path of an airborne system. From an understanding of fixed system placement for maximum performance and in keeping with the control of the previous point spread function analysis, circular and linear arrangements of the transmitter and receiver combinations were selected.

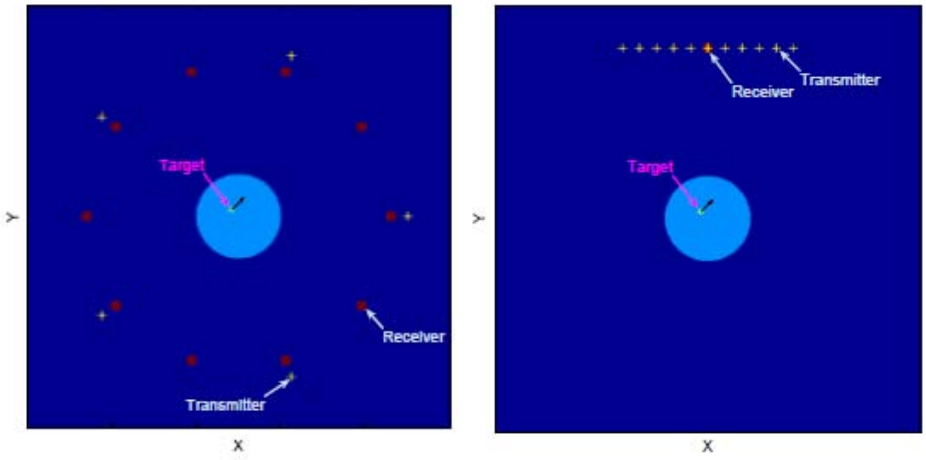

Figure 18. Transmitter/Receiver Arrangements Used in Analysis

Another input to the GUI is the number of targets with their respective position and velocity. The targets were varied in position with constant velocity and then varied in velocity with fixed positions. This arrangement was the same for each of the selected

waveforms. The emphasis of the GUI was to determine the imaging system capabilities associated with various imaging system parameters. The goal was to show that certain parameters give better results than other parameters and put metrics on that comparison.

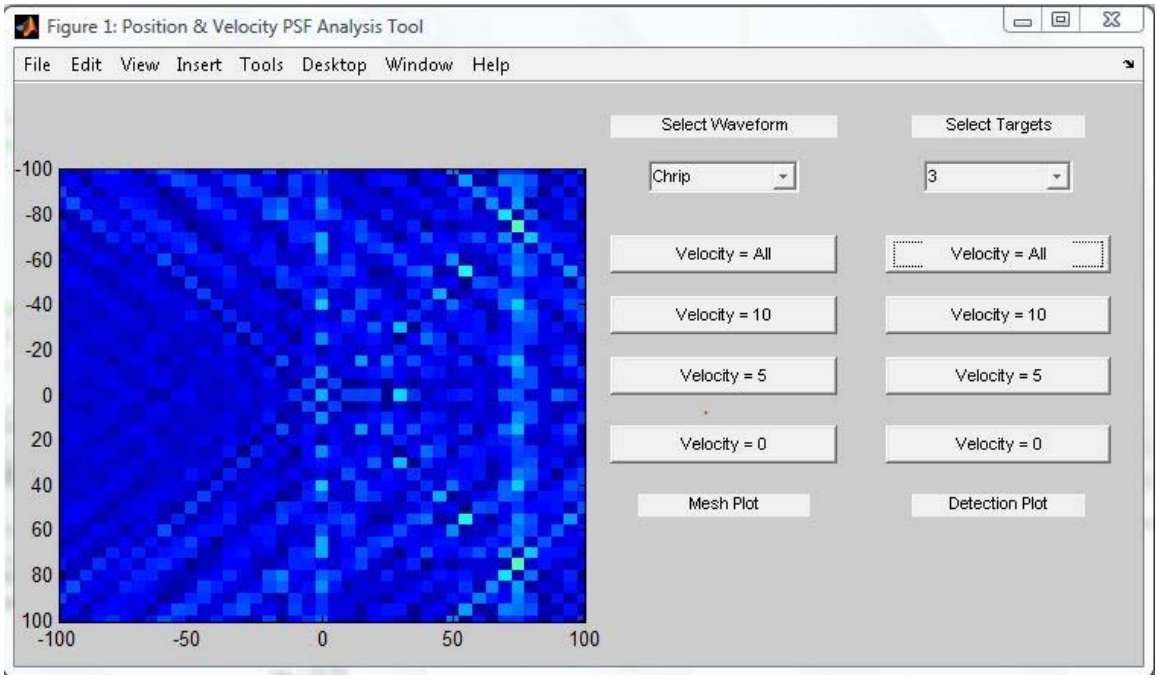

Figure 19. Screen Shot of GUI with Chirp Pulse and Three Point Targets

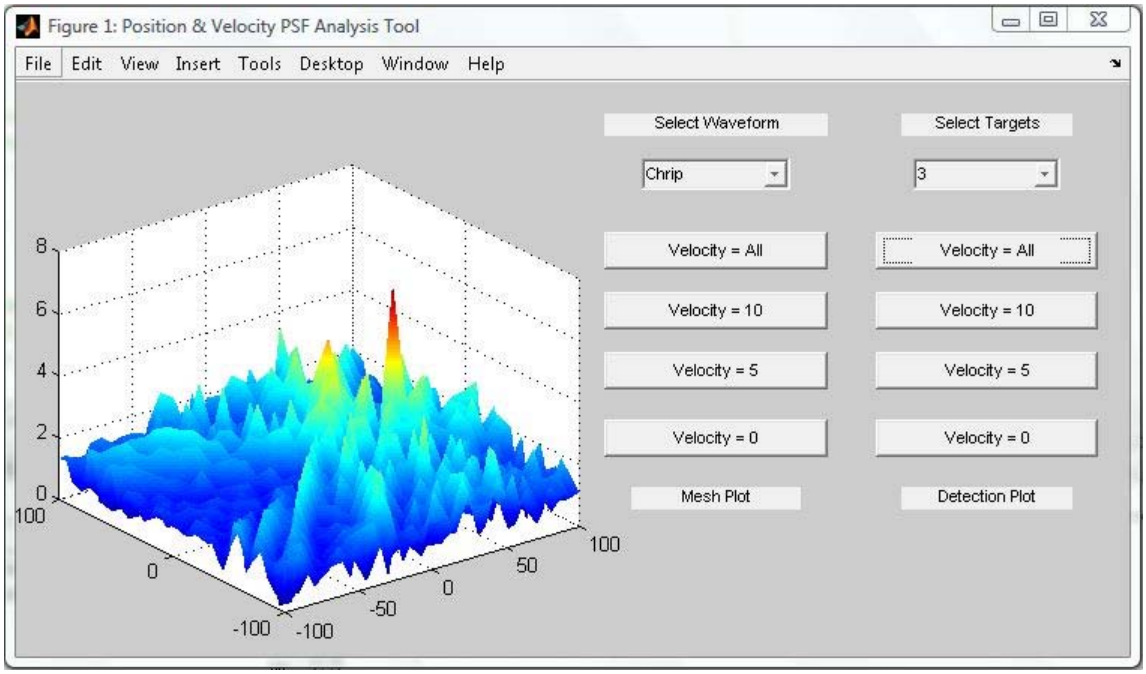

Figure 20. Screen Shot of GUI with Chirp Pulse and Three Point Targets

Point targets were used to perform image analysis for the set of parameters being examined. The SAR imaging system is linear and it is useful to characterize it performance through its impulse response. In general, the impulse response for an imaging system is obtained by measuring the system response to a single, isolated scatter. A small, discrete scatterer is called a point target. Many important image quality parameters can be estimated from measurements made on the point target response [8]. An approach for analysis is to treat the processed image of the point target as a sinc-like function [8] The most important quality parameters, i.e., metrics for image quality, are the impulse response width that defines the image resolution and the peak or integrated sidelobe ratio that pertains to the image contrast [8]. This is has been displayed for the test analysis in Figure 21.

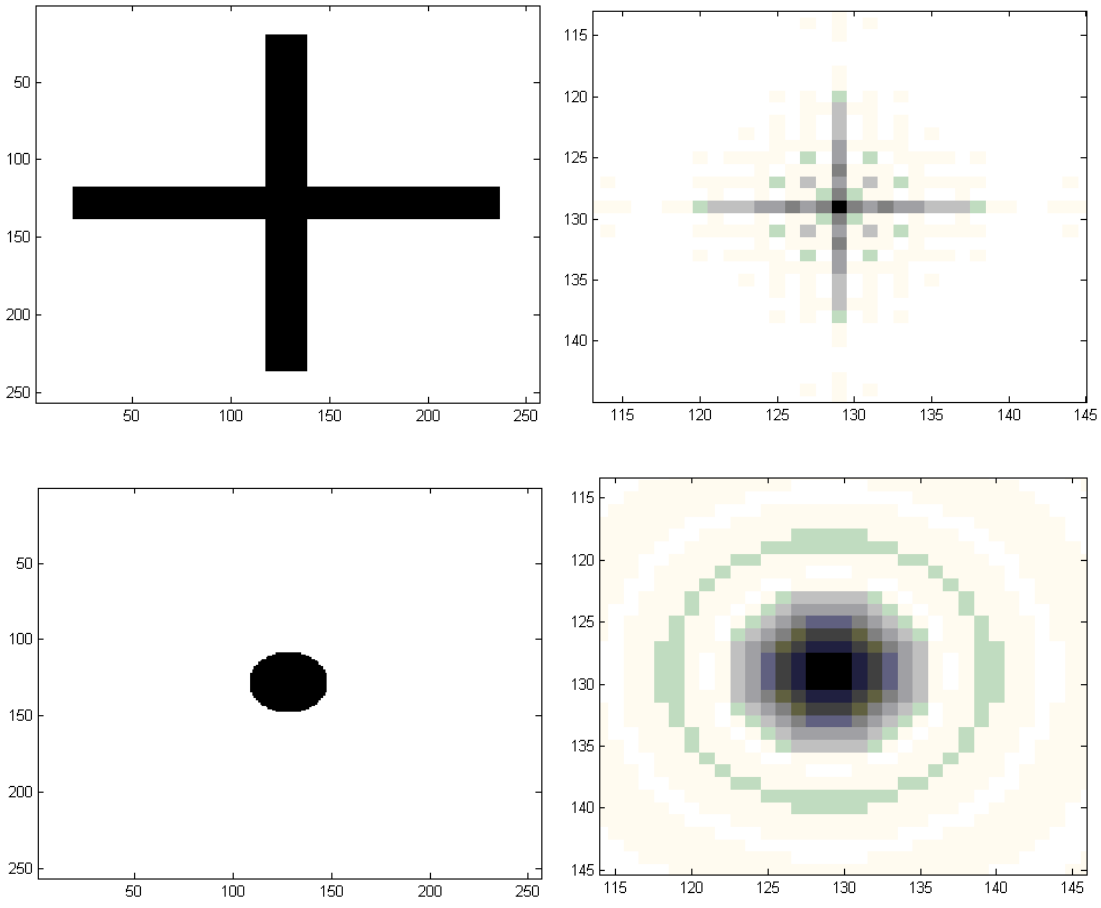

Figure 21. Test cases of two-dimensional point target analysis

The figures above were analyzed by evaluating the point target response of the imaging system. In order to measure these parameters, the point target response must be interpolated in the vicinity of the peak. The peak is usually contained within one or two pixels in the processed data. The process was to establish a window of n x n samples centered on the peak then with zero-padding performs a sinc-like interpolator by the FFT. The contour plots of the point targets peak of the expanded point target energy are shown on the right (Figure20).

The previously described approach is not applicable to the imaging of moving targets. For the case of moving targets, the velocities of targets will be restricted to two dimensions and thus the point spread function is four-dimensional. This adds complexity to the display of the data and is the reason for the Graphical User Interface and its ability to switch between the *surf* plot and *imagesc* display of a data set. These displays will be used to determine the level of accuracy for the imaging system configurations as well as the artifacts for that configuration.

D. ACTUAL DATA ANALYSIS

In addition to the development of the Graphical User Interface, there was a need for a baseline imaging process for comparison during development the phase space algorithm. In order to create this baseline, the imaging program ENVI was utilized to analyze unclassified and classified data sets. ENVI is a very capable imaging program for radar as it was designed for image analysis and all its processing functions are inherently radar capable including all display capabilities, stretching, color manipulations, and classification. ENVI provides standard and advanced tools for analysis of detected radar images as well as advanced SAR systems such as JPL's AIRSAR and SIR-C systems. ENVI can process many different imaging system's data such as ERS-1/ERS-2, JERS-1, RADARSAT, X-SAR and AIRSAR data as well as any other detected SAR data set. In addition, ENVI is designed to handle radar data distributed in the CEOS format, and should be able to handle data from other radar systems that distribute their data in this format [10].

The ENVI program was used to analyze SIR-C data from collections over Germany and Hawaii. The program has a Radar menu that allows the user to select the imaging system that was used to collect the data and then applies the proper reader file to that data. After opening the data files, some imaging systems require that the data be synthesized, or converted to the proper format, such is the case for Lynx SAR data. ENVI has a specific tool that will calibrate the Beta Naught and Sigma Naught for the imaging system. The Beta Naught (β^0) is used to calibrate the brightness and the Sigma Naught (σ^0) is used to calibrate the data to a radar backscatter coefficient. The Sigma Naught calibration requires that the data correspond to imaging system incidence angles and absolute correlation values. These values are not always available with the various data sets and thus the calibration can be significantly altered.

ENVI was used to determine possible unclassified data sets for exploitation with the phase space algorithm. The following images are from a data set that was collected by SIR-C imaging system. SIR-C is the shuttle imaging radar-C band. The imaging system shows large features such as runways and coastline. Large buildings can be seen as well (Figure 24).

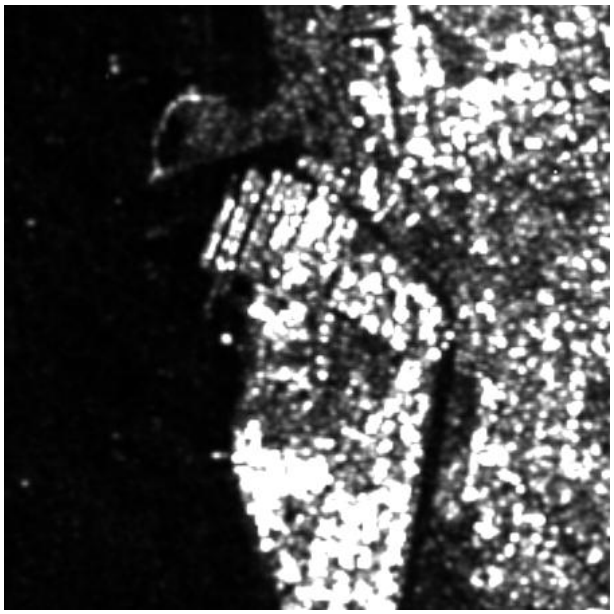

Figure 22. SIR-C HH data showing large urban area

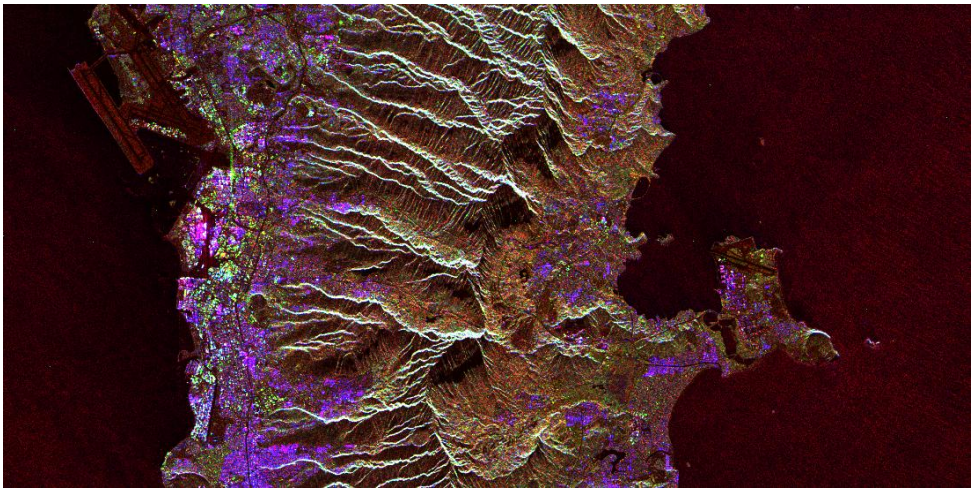

Figure 23. SIR-C data with color enhancement of Oahu

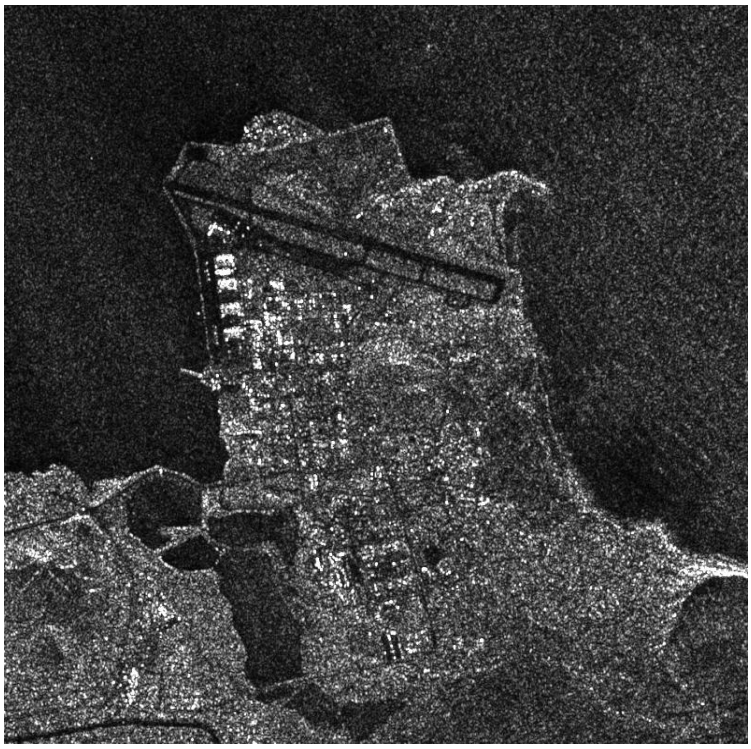

Figure 24. SIR-C ENVI processed image showing runway at MCBH Kaneohe Bay

These images did not yield the information that would support the phase space imaging analysis due to the resolution issues and lack of target motion due to such coarse resolution.

THIS PAGE INTENTIONALLY LEFT BLANK

V. RESULTS AND CONCLUSION

A. IMAGING RESULTS FOR TEST DATA

1. Target Imaging in Velocity Space

The imaging of point targets with the phase space algorithm showed very good results. The imaging system analysis proved that the targets are mapped to a position in the imaging scene with the correct velocity. The challenge becomes which set of imaging system parameters yields the best results. The following table describes the set of parameters evaluated.

Waveform	Transmitter / Receiver Configuration	# of Targets
Rectangular Pulse	Four Corners	1–4
	Linear	1–4
	U Shape	1
Chirp Pulse	Four Corners	1–4
	Linear	1–4
	U Shape	1

Figure 25. Evaluated Imaging System Parameter Table of Variables

The imaging system parameters were developed to have a real world applications associated with the transmitter and receiver locations. The long linear array would represent the ScanSar mode of aircraft or satellite imaging systems. The U shaped array of transmitter and receiver locations would represent a typical formation of naval vessels. The final configuration that was analyzed would be representative of the minimum number or stationary receivers needed for adequate imaging. The above cases were analyzed with varying waveforms and varying number of targets.

Point target analysis was utilized to apply metrics to the analysis of the imaging system performance for the variety of input parameters. The following plots show the

various imaging system performance capabilities. The results show that the targets can be imaged appropriately with velocity and proper position.

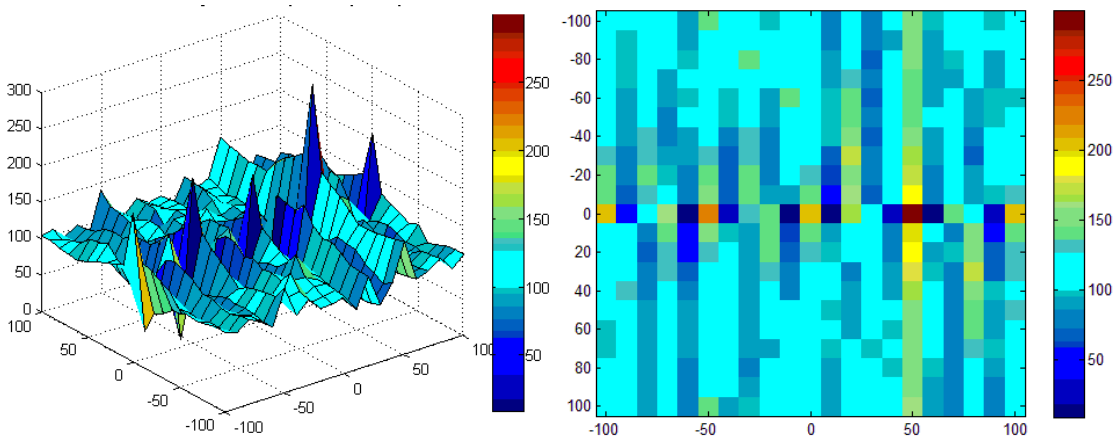

Figure 26. Chirp Pulse, Four Corner Transmitters/Receivers with 1 Target moving at a velocity (-10,0).

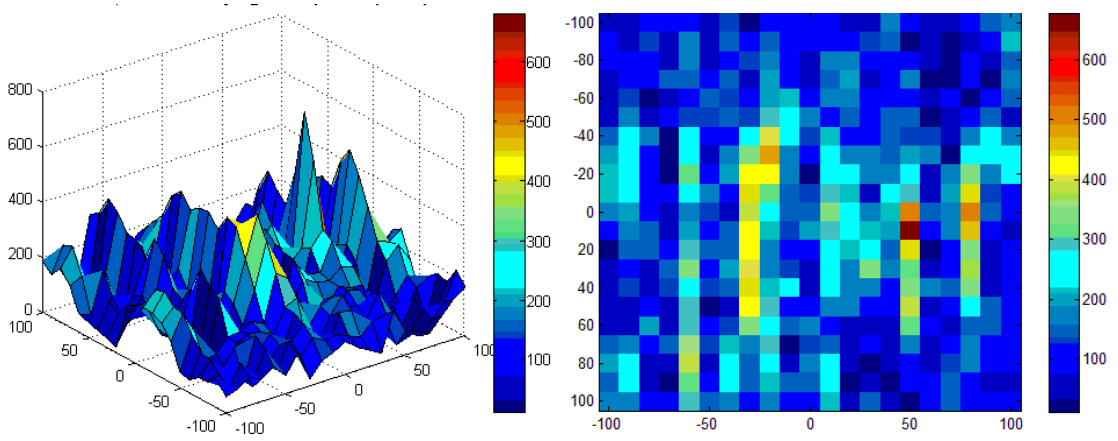

Figure 27. Chirp Pulse, Linear Array 8 Transmitters/ 21 Receivers with 1 Target moving at a velocity (-10,0).

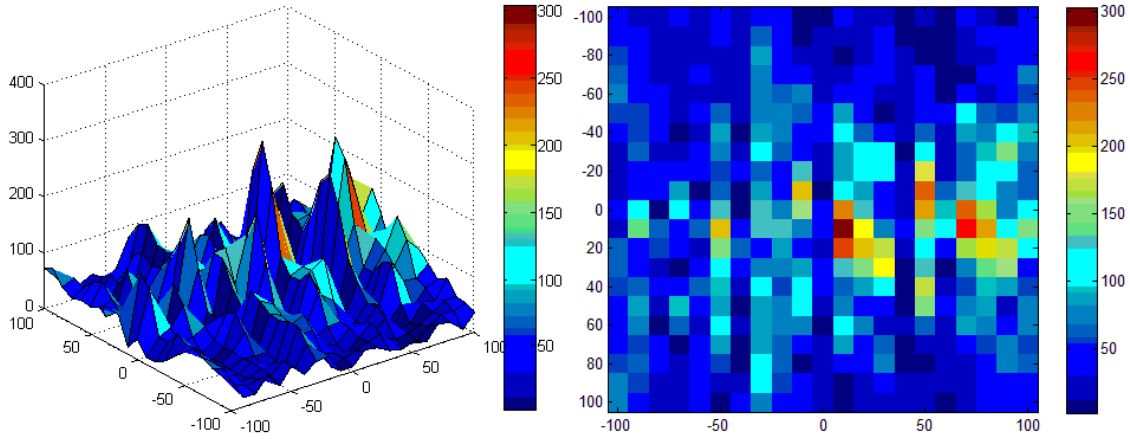

Figure 28. Chirp Pulse, U Shaped Array 4 Tr/ 4 Rec with 1 Target moving at a velocity (-10,0).

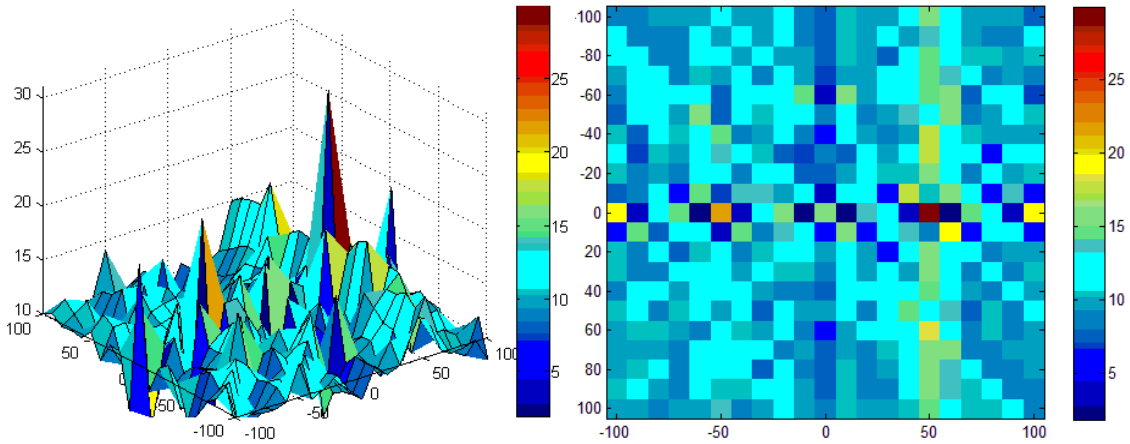

Figure 29. Rect Pulse, Four Corner Transmitters/Receivers with 1 Target moving at a velocity (-10,0).

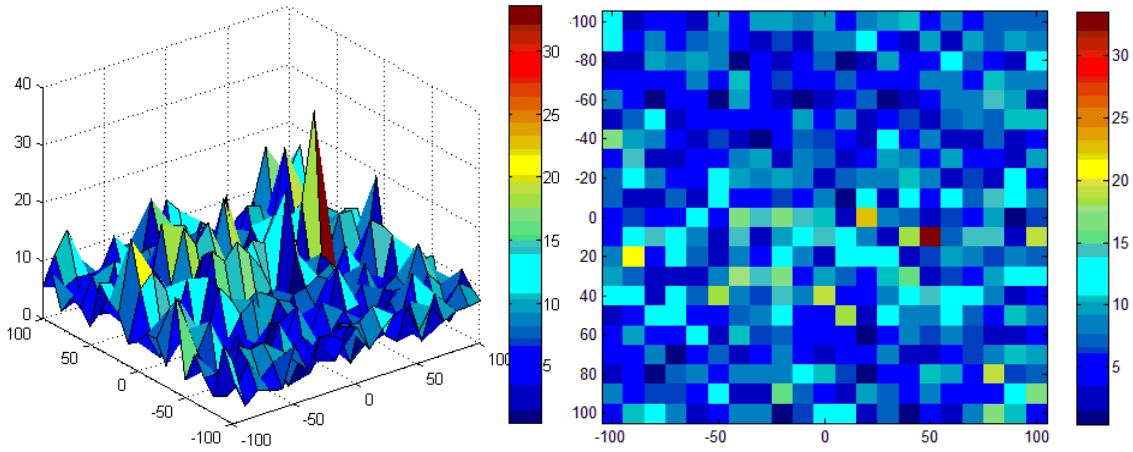

Figure 30. Rect Pulse, Linear Array 8 Transmitters/ 21 Receivers with 1 Target moving at a velocity (-10,0).

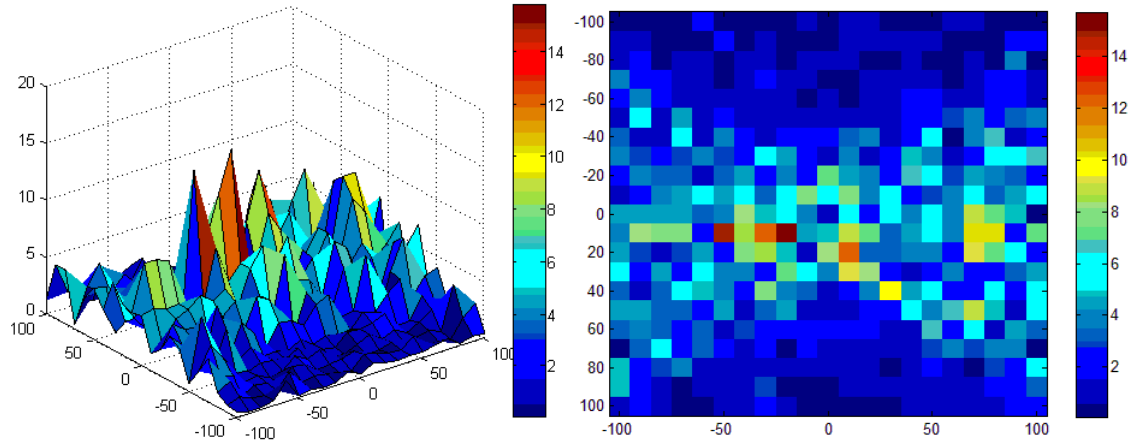

Figure 31. Rect Pulse, U-Shaped Array 4 Txs/ 4 Receivers with 1 Target moving at a velocity (-10,0).

The results show that the linear array, as well as the four corner position array, image the target appropriately. The figures also show the expected artifacts from each of these analysis cases. Imaging artifacts will be displayed with point targets just as the artifacts will be displayed when being applied to real data sets. There is just as much to learn about where the target is not and what the noise floor is based on that imaging system scenario. The U shaped array did not perform particularly well, as it was not able to isolate a single point target. The level of artifacts in the U shaped array image shows that the target is being confused with non-target related artifacts.

B. IMAGING RESULTS FOR REAL DATA

1. Target Imaging in Velocity Space

The analysis that was accomplished on real data sets was limited for a number of reasons. Adjunct analysis of imaging system requirements for the phase space algorithm has shown that randomness in the collection profile of the imaging system improves the processed image output. This is in stark contrast to the typical collection profile of current imaging systems. RadarSatII cannot perform random maneuvers on its orbital trajectory. The majority of airborne systems try to maintain a stable platform to reduce oscillations in the image caused by the aircraft. The turntable used to acquire ISAR of the backhoe did not provide any randomness for the collection of the data. Secondly, the backhoe data is from a stationary target. In addition to the zero Doppler effect, there are unknowns about the collection, such as range to target as well as pulse width of the imaging system. These factors contributed to the poor image capabilities of the phase space algorithm.

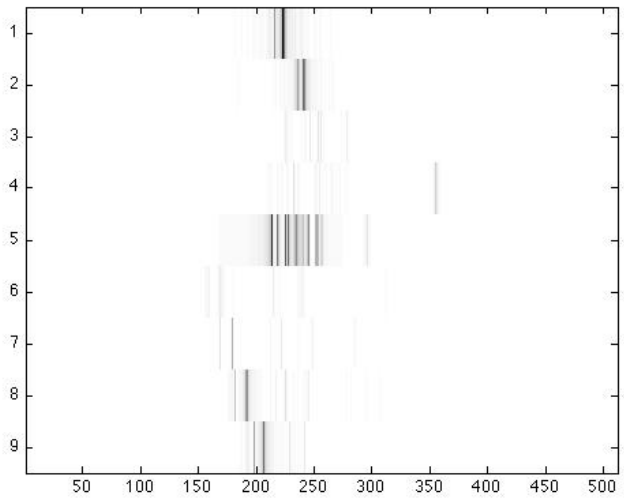

Figure 32. IFFT of data set from Backhoe collection.
Data provided by DARPA.

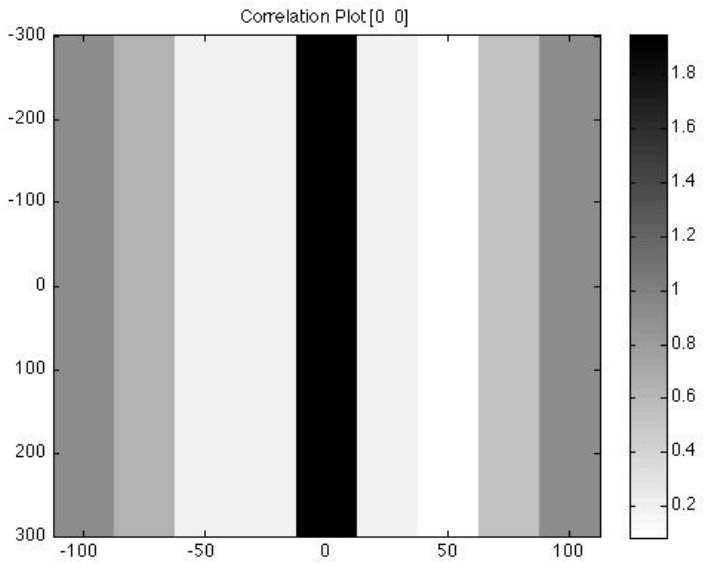

Figure 33. Correlation plot of target at (0,0) Velocity and Position(0,0)

C. FUTURE WORK

This project has moved forward significantly with the volume of work completed by the SAR Imagery Research Team during the summer and fall quarters of the 2009 academic year at the Naval Postgraduate School. The future work that is required will refine the algorithms and techniques to improve the imaging of moving targets. The work needs to incorporate interaction with fleet users for asymmetric collections of data that will support the randomness assertions for improvement of imaging quality.

D. CONCLUSION

The significance of the ability to image moving targets with Synthetic Aperture Radar systems cannot be overstated as a vital tool in the commander's arsenal for battle space awareness. This project has shown that imaging of moving targets with Synthetic Aperture Radar has been demonstrated on point targets with various velocities. The point target analysis has been accomplished to show imaging system capabilities for different, real world applications of imaging systems. The image artifacts have been shown for various imaging system configurations for real world collection platforms. A statistical approach was taken to show these configuration parameters capabilities and begin to design a set of parameters that will best exploit the phase space algorithm. The work to

date, is a collaboration of efforts and future work will leverage the gains made to improve capabilities of existing imaging systems with the development of improved algorithms for increased capabilities.

THIS PAGE INTENTIONALLY LEFT BLANK

APPENDIX

A. MATLAB CODE FOR PERFECTLY CONDUCTING SPHERE

```
%  A plane harmonic wave of frequency w (with k = w/c) and traveling along the
%  z-axis is incident on a perfectly conducting sphere of radius a. Determine the
%  physical optics contribution to the scattered field and the associated scattering
%  cross-section of the sphere. Plot this cross-section on a log-log plot as a
%  function of ka (i.e., compare this result to figure 3.2 of the class notes).

format long e
syms K a
K = .01:.0001:10;
a = 1;

x = K;
y = ((pi.*a.^2)./(K.^2)).*(K.^2 + 1/2 - (1/2*(cos(2.*K))) - K.*sin(2.*K));
loglog(x,y,'.');
grid
xlabel('ka');
ylabel('SIGMA');
title('Hpo Contribution to Scattered Field of Cross Section of Sphere');
```

B. MATLAB CODE FOR POINT TARGET ANALYSIS

```
clear
N=256;
a=-10; b=10; dx=(b-a)/(N-1);
x=[a:dx:b];

%%%%% Rect Func with width  w=10   %%%%%
k1 = zeros(1,N); w=.1*(b-a);
k1(floor((N-w/dx)/2):floor((N+w/dx)/2))=1;
plot(x,k1); pause
K1=fft(k1);
plot(abs(K1)); pause
K1=fftshift(K1);
plot(abs(K1)); pause

%%%%% Rect func of width w = 50%    %%%%%%
k1 = zeros(1,N); w=.5*(b-a);
k1(floor((N-w/dx)/2):floor((N+w/dx)/2))=1;
plot(x,k1); pause
K1=fft(k1);
plot(abs(K1)); pause
K1=fftshift(K1);
plot(abs(K1)); pause

%%  Object Function
subplot(1,1,1)
M=N;
```

```
ff=zeros(N,M);
ff(N/2-10:N/2+10,20:M-20)=1;
ff(20:N-20,M/2-10:M/2+10)=1;
colormap(gray);
imagesc(ff); pause
FF=fftshift(fft2(ff));
imagesc(abs(FF)); pause

%%%%%  2-D Kernal   %%%%%%
kk=zeros(N,M);
R=20;
for m=1:M
   for n=1:N
      if (N/2-n)^2+(M/2-m)^2<R^2
           kk(n,m)=1;
      end
      %end
   end
end
imagesc(kk); pause
KK=fftshift(fft2(kk));
imagesc(abs(KK)); pause

%%%%%  2D Convolution  %%%%%
GG=KK.*FF;
gg=ifftshift(ifft2(GG));
imagesc(abs(gg))
```

C. MATLAB CODE FOR IMAGE ANALYSIS OF MOVING TARGETS

Chirp Signal, One Target, One Transmitter and Four Receivers

```
close all
clear all
clc
%Origin of the image scene is set at (0,0)
%Target is set at (1km,1km) away from the origin with Velocity of (1,0)
%Transmitted is set at (-10km,0) away from the origin
%format long e
%Target Information
N_tt=1;        %No of Targets
tt=[200 50];     %Target X position, Y position
tt_vel=[-10 0];   %Target velocity in X direction, Y direction

%Transmitter Information
N_Tx=4;        %No of Transmitter
Tx =[-10e3 -10e3;-10e3 10e3;10e3 -10e3;10e3 10e3];    %Transmitter X position, Y position
T_tx=0;          %Start time of transmitted pulse = always zero for the case of single transmitter
Tx_mag= sqrt(Tx(:,1).*Tx(:,1)+Tx(:,2).*Tx(:,2));
Tx_hat(:,1)= Tx(:,1)./sqrt(Tx(:,1).*Tx(:,1)+Tx(:,2).*Tx(:,2));
Tx_hat(:,2)= Tx(:,2)./sqrt(Tx(:,1).*Tx(:,1)+Tx(:,2).*Tx(:,2));

%Receiver Information
N_Rx=4;
```

```
Rx=[-10e3 -10e3;10e3 10e3;-10e3 10e3;10e3 -10e3];    %Receiver X position, Y position
Rx_mag= sqrt(Rx(:,1).*Rx(:,1)+Rx(:,2).*Rx(:,2));
Rx_hat(:,1)=Rx(:,1)./sqrt(Rx(:,1).*Rx(:,1)+Rx(:,2).*Rx(:,2));
Rx_hat(:,2)= Rx(:,2)./sqrt(Rx(:,1).*Rx(:,1)+Rx(:,2).*Rx(:,2));

%Signal information
c=3e8;
W_tx=2*pi*(10e9);      %Carrier Freq is 10GHz
K_tx=W_tx/c;          %Ky=Wy/c

%Waveform information
%pulse width of 0.2 us (30m of resolution and listening time of 100us (15km of Runamb)
% total period 100us

fs = 20e6;              % Using baseband signal of 1kHz. Therefore 20MHz sampling. Nyquisting sampling
rate
ts = 1/fs;
t1 = 0:1:20;           %0:ts:1e-6; %0:1:20;    %pusle transmit time
t2 = 0:1:1979;          %1e-6+ts:ts:100e-6;     %0:1:1979;              %listening time
period = 100e-6;
T_period=0:ts:100e-6;
T=[t1 t2 t1 t2 t1 t2];              %period of 100us
for n = 1:1:(length(T_period))
   if n <= (20)
      j = 1-(n/20);
      s(:,n)=j;
   end
   if n > (20)
      j = 0;
      s(:,n)=j;
   end
end
sp = [s s s];
S=fft(sp);
w=(2*pi/period)*T;

TT_Data=zeros(1,length(sp));

%Generating Target Signal
for l=1:N_Tx    %For all Transmitter
   for m=1:N_Rx    %For all Receiver
      for n=1:N_tt       %For all targets
         tau= T_tx+(((Tx_mag(l,:)-(Tx_hat(l,:)*tt(n,:)'))+(Rx_mag(m,:)-(Rx_hat(m,:)*tt(n,:)')))/c);%time
delay
         phi=K_tx*Rx_mag(m,:)-K_tx*(Tx_hat(l,:)+Rx_hat(m,:))*(tt(n,:)+((Rx_hat(m,:)*(Rx(m,:)-
tt(n,:))')*tt_vel/c))';
         alpha=1-(Tx_hat(l,:)+Rx_hat(m,:))*(tt_vel/c)';
         TT_Data = TT_Data + exp(i*phi)*exp(i*W_tx*alpha*T).*ifft(S.*exp(-i*w*tau));
      end
   end
end
% figure
% plot(T_period,abs(TT_Data));
```

```
%Expected Target Position
E_tt_x=-1e3:10:1e3;     %Sampled by Range Resolution
E_tt_y=-1e3:10:1e3;     %Sampled by Range Resolution
E_tt_y=fliplr(E_tt_y);

%Expected Target Velocity
E_tt_vel_x= -10;
E_tt_vel_y= 0;
E_tt_vel_y=fliplr(E_tt_vel_y);
% E_tt_vel=[-10 0];

L=length(E_tt_y)*length(E_tt_x);



for u=1:length(E_tt_vel_y)
   for v=1:length(E_tt_vel_x)
      E_tt_vel=[E_tt_vel_x(1,v) E_tt_vel_y(1,u)];

%Generating Expected Target Database
for g=1:length(E_tt_y)
   for h=1:length(E_tt_x)
      E_tt=[E_tt_x(1,h) E_tt_y(1,g)];
      E_TT_Data=zeros(1,length(T));
      for l=1:N_Tx    %For all Transmitter
         for m=1:N_Rx    %For all Receiver
            tau= T_tx+(((Tx_mag(l,:)-(Tx_hat(l,:)*E_tt(1,:)'))+(Rx_mag(m,:)-(Rx_hat(m,:)*E_tt(1,:)')))/c);
%time delay
            phi=K_tx*Rx_mag(m,:)-K_tx*(Tx_hat(l,:)+Rx_hat(m,:))*(E_tt(:,1)+((Rx_hat(m,:)*(Rx(m,:)-
E_tt(:,n))')*E_tt_vel/c))';
            alpha=1-(Tx_hat(l,:)+Rx_hat(m,:))*(E_tt_vel/c)';
            E_TT_Data = E_TT_Data + exp(i*phi)*exp(i*W_tx*alpha*T).*ifft(S.*exp(-i*w*tau));
         end
      end
      I(g,h)=E_TT_Data*TT_Data';
   end
end

figure
%clims = [0 200];
surf(E_tt_x,E_tt_y,abs(I))
title(['velocity Vector [', num2str(E_tt_vel),']']);
colorbar;
   end
end
```

Chirp Signal, One Target, Eight Transmitters and Twenty One Receivers

```
close all
clear all
clc
%Origin of the image scene is set at (0,0)
```

```
%Target is set at (1km,1km) away from the origin with Velocity of (1,0)
%Transmitted is set at (-10km,0) away from the origin
%format long e

%Target Information
N_tt=1;         %No of Targets
tt=[50 10];     %Target X position, Y position
tt_vel=[-10 0];   %Target velocity in X direction, Y direction

%Transmitter Information
N_Tx=8;         %No of Transmitter
Tx =[-10e3 -10e3;-7e3 -10e3;-5e3 -10e3;-2e3 -10e3;2e3 -10e3;5e3 -10e3;7e3 -10e3;10e3 -10e3];
%Transmitter X position, Y position
T_tx=0;           %Start time of transmitted pulse = always zero for the case od single transmitter
Tx_mag= sqrt(Tx(:,1).*Tx(:,1)+Tx(:,2).*Tx(:,2));
Tx_hat(:,1)= Tx(:,1)./sqrt(Tx(:,1).*Tx(:,1)+Tx(:,2).*Tx(:,2));
Tx_hat(:,2)= Tx(:,2)./sqrt(Tx(:,1).*Tx(:,1)+Tx(:,2).*Tx(:,2));

%Receiver Information
N_Rx=21;
Rx=[-10e3 -10e3;-9e3 -10e3;-8e3 -10e3;-7e3 -10e3;-6e3 -10e3;-6e3 -10e3;...
   -5e3 -10e3;-4e3 -10e3;-3e3 -10e3;-2e3 -1e3;0 -10e3;1e3 -10e3;2e3 -10e3;...
   3e3 -10e3;4e3 -10e3;5e3 -10e3;6e3 -10e3;7e3 -10e3;8e3 -10e3;9e3 -10e3;13 -10e3];    %Receiver X
position, Y position



Rx_mag= sqrt(Rx(:,1).*Rx(:,1)+Rx(:,2).*Rx(:,2));
Rx_hat(:,1)=Rx(:,1)./sqrt(Rx(:,1).*Rx(:,1)+Rx(:,2).*Rx(:,2));
Rx_hat(:,2)= Rx(:,2)./sqrt(Rx(:,1).*Rx(:,1)+Rx(:,2).*Rx(:,2));

%Signal information
c=3e8;
W_tx=2*pi*(10e9);       %Carrier Freq is 10GHz
K_tx=W_tx/c;          %Ky=Wy/c

%Waveform information
%pulse width of 0.2 us (30m of resolution and listening time of 100us (15km of Runamb)
% total period 100us

fs = 20e6;              % Using baseband signal of 1kHz. Therefore 20MHz sampling. Nyquisting sampling
rate
ts = 1/fs;
t1 = 0:1:20;           %0:ts:1e-6; %0:1:20;    %pusle transmit time
t2 = 0:1:1979;         %1e-6+ts:ts:100e-6;     %0:1:1979;             %listening time
period = 100e-6;
T_period=0:ts:100e-6;
T=[t1 t2 t1 t2 t1 t2];             %period of 100us
for n = 1:1:(length(T_period))
   if n <= (20)
      j = 1-(n/20);
      s(:,n)=j;
   end
   if n > (20)
```

```
        j = 0;
        s(:,n)=j;
    end
end
sp = [s s s];
S=fft(sp);
w=(2*pi/period)*T;

TT_Data=zeros(1,length(sp));

%Generating Target Signal
for l=1:N_Tx    %For all Transmitter
    for m=1:N_Rx    %For all Receiver
        for n=1:N_tt        %For all targets
            tau= T_tx+(((Tx_mag(l,:)-(Tx_hat(l,:)*tt(n,:)'))+(Rx_mag(m,:)-(Rx_hat(m,:)*tt(n,:)')))/c);%time
delay
            phi=K_tx*Rx_mag(m,:)-K_tx*(Tx_hat(l,:)+Rx_hat(m,:))*(tt(n,:)+((Rx_hat(m,:)*(Rx(m,:)-
tt(n,:))')*tt_vel/c))';
            alpha=1-(Tx_hat(l,:)+Rx_hat(m,:))*(tt_vel/c)';
            TT_Data = TT_Data + exp(i*phi)*exp(i*W_tx*alpha*T).*ifft(S.*exp(-i*w*tau));
        end
    end
end

%Expected Target Position
E_tt_x=-1e2:10:1e2;     %Sampled by Range Resolution
E_tt_y=-1e2:10:1e2;     %Sampled by Range Resolution
E_tt_y=fliplr(E_tt_y);

%Expected Target Velocity
E_tt_vel_x= -10;
E_tt_vel_y= 0;
E_tt_vel_y=fliplr(E_tt_vel_y);
% E_tt_vel=[-10 0];

L=length(E_tt_y)*length(E_tt_x);

for u=1:length(E_tt_vel_y)
    for v=1:length(E_tt_vel_x)
        E_tt_vel=[E_tt_vel_x(1,v) E_tt_vel_y(1,u)];

%Generating Expected Target Database
for g=1:length(E_tt_y)
    for h=1:length(E_tt_x)
        E_tt=[E_tt_x(1,h) E_tt_y(1,g)];
        E_TT_Data=zeros(1,length(T));
        for l=1:N_Tx    %For all Transmitter
            for m=1:N_Rx    %For all Receiver
                tau= T_tx+(((Tx_mag(l,:)-(Tx_hat(l,:)*E_tt(1,:)'))+(Rx_mag(m,:)-(Rx_hat(m,:)*E_tt(1,:)')))/c);
%time delay
                phi=K_tx*Rx_mag(m,:)-K_tx*(Tx_hat(l,:)+Rx_hat(m,:))*(E_tt(:,1)+((Rx_hat(m,:)*(Rx(m,:)-
E_tt(:,n))')*E_tt_vel/c))';
                alpha=1-(Tx_hat(l,:)+Rx_hat(m,:))*(E_tt_vel/c)';
```

```
            E_TT_Data = E_TT_Data + exp(i*phi)*exp(i*W_tx*alpha*T).*ifft(S.*exp(-i*w*tau));
          end
        end
        I(g,h)=E_TT_Data*TT_Data';
    end
end
figure
%clims = [0 200];
imagesc(E_tt_x,E_tt_y,abs(I))
title(['U Shape 8T/21R 1 Target @ Velocity Vector [', num2str(E_tt_vel),']']);
colorbar;
end
```

Rect Signal, One Target, One Transmitter and Four Receivers

```
close all
clear all
clc

%Origin of the image scene is set at (0,0)
%Target is set at (1km,1km) away from the origin with Velocity of (1,0)
%Transmitted is set at (-10km,0) away from the origin

%format long e

%Target Information
N_tt=1;         %No of Targets
tt=[50 10];     %Target X position, Y postion
tt_vel=[-10 0];   %Target velocity in X direction, Y direction

%Transmitter Information
N_Tx=3;         %No of Transmitter
Tx =[-10e3 -10e3;10e3 10e3;-10e3 10e3];    %Transmitter X position, Y position
T_tx=0;           %Start time of transmitted pulse = always zero for the case od single transmitter
Tx_mag= sqrt(Tx(:,1).*Tx(:,1)+Tx(:,2).*Tx(:,2));
Tx_hat(:,1)= Tx(:,1)./sqrt(Tx(:,1).*Tx(:,1)+Tx(:,2).*Tx(:,2));
Tx_hat(:,2)= Tx(:,2)./sqrt(Tx(:,1).*Tx(:,1)+Tx(:,2).*Tx(:,2));

%Receiver Information
N_Rx=4;
Rx=[-10e3 -10e3;10e3 10e3;-10e3 10e3;10e3 -10e3];    %Receiver X position, Y position
Rx_mag= sqrt(Rx(:,1).*Rx(:,1)+Rx(:,2).*Rx(:,2));
Rx_hat(:,1)=Rx(:,1)./sqrt(Rx(:,1).*Rx(:,1)+Rx(:,2).*Rx(:,2));
Rx_hat(:,2)= Rx(:,2)./sqrt(Rx(:,1).*Rx(:,1)+Rx(:,2).*Rx(:,2));

% Rx_mag = sqrt(sum((Rx.^2)'))';
% Rx_hat(:,1) = (Rx(:,1)'./sqrt(sum((Rx.^2)')))';
% Rx_hat(:,2) = (Rx(:,2)'./sqrt(sum((Rx.^2)')))';

%Signal information
c=3e8;
W_tx=2*pi*(10e9);       %Carrier Freq is 10GHz
K_tx=W_tx/c;          %Ky=Wy/c
```

```
%Waveform information
%pulse width of 0.2 us (30m of resolution and listening time of 100us (15km of Runamb)
% total period 100us

fs = 20e6;                          % Using baseband signal of 1kHz. Therefore 20MHz sampling. Nyquisting
sampling rate
ts = 1/fs;
t1 = 0:1:20; %0:ts:1e-6; %0:1:20;                       %pusle transmit time
t2 = 0:1:1979; %1e-6+ts:ts:100e-6; %0:1:1979;               %listening time
period = 100e-6;
T_period=0:ts:100e-6;
T=[t1 t2];                          %period of 100us
s = [rectpuls(t1) zeros(1,length(t2))]; % 0.2 us Rect. pulse
S=fft(s);
w=(2*pi/period)*T;

TT_Data=zeros(1,2001);
%Generating Target Signal
for l=1:N_Tx    %For all Transmitter
   for m=1:N_Rx    %For all Receiver
      for n=1:N_tt       %For all targets
         tau= T_tx+(((Tx_mag(l,:)-(Tx_hat(l,:)*tt(n,:)'))+(Rx_mag(m,:)-(Rx_hat(m,:)*tt(n,:)')))/c);%time
delay
         phi=K_tx*Rx_mag(m,:)-K_tx*(Tx_hat(l,:)+Rx_hat(m,:))*(tt(n,:)+((Rx_hat(m,:)*(Rx(m,:)-
tt(n,:))')*tt_vel/c))';
         alpha=1-(Tx_hat(l,:)+Rx_hat(m,:))*(tt_vel/c)';
         TT_Data = TT_Data + exp(i*phi)*exp(i*W_tx*alpha*T).*ifft(S.*exp(-i*w*tau));
      end
   end
end

% figure
% plot(T_period,abs(TT_Data));

%Expected Target Position
E_tt_x=-1e2:10:1e2;     %Sampled by Range Resolution
E_tt_y=-1e2:10:1e2;     %Sampled by Range Resolution
E_tt_y=fliplr(E_tt_y);

%Expected Target Velocity
E_tt_vel_x= -10;
E_tt_vel_y= 0;
E_tt_vel_y=fliplr(E_tt_vel_y);
% E_tt_vel=[-10 0];

L=length(E_tt_y)*length(E_tt_x);


for u=1:length(E_tt_vel_y)
   for v=1:length(E_tt_vel_x)
      E_tt_vel=[E_tt_vel_x(1,v) E_tt_vel_y(1,u)];
```

```
%Generating Expected Target Database
for g=1:length(E_tt_y)
   for h=1:length(E_tt_x)
      E_tt=[E_tt_x(1,h) E_tt_y(1,g)];
      E_TT_Data=zeros(1,length(T));
      for l=1:N_Tx    %For all Transmitter
         for m=1:N_Rx    %For all Receiver
            tau= T_tx+(((Tx_mag(l,:)-(Tx_hat(l,:)*E_tt(1,:)'))+(Rx_mag(m,:)-(Rx_hat(m,:)*E_tt(1,:)')))/c);
%time delay
            phi=K_tx*Rx_mag(m,:)-K_tx*(Tx_hat(l,:)+Rx_hat(m,:))*(E_tt(:,1)+((Rx_hat(m,:)*(Rx(m,:)-
E_tt(:,n))')*E_tt_vel/c))';
            alpha=1-(Tx_hat(l,:)+Rx_hat(m,:))*(E_tt_vel/c)';
            E_TT_Data = E_TT_Data + exp(i*phi)*exp(i*W_tx*alpha*T).*ifft(S.*exp(-i*w*tau));
         end
      end
      I(g,h)=E_TT_Data*TT_Data';
   end
end
figure
%subplot(2,2,3);
%clims = [0 200];
imagesc(E_tt_x,E_tt_y,abs(I))
%axis([-100 100 -100 100 10 31])
title(['velocity Vector [', num2str(E_tt_vel),']']);
colorbar;
   end
end
```

THIS PAGE INTENTIONALLY LEFT BLANK

LIST OF REFERENCES

[1] "Radar" class notes for PH4272, Department of Physics, United States Naval Postgraduate School, 2008.

[2] Canada Centre for Remote Sensing, "Tutorial: Radar Remote Sensing", *GlobeSAR Program, Canada Centre for Remote Sensing, Natural Resources Canada*, Sept. 25 2007[Online]. Available: http://ccrs.nrcan.gc.ca/org/programs/globesar/index.php. [Accessed: August 17, 2009].

[3] C. Oliver and S. Quegan, *Understanding Synthetic Aperture Radar Images*, Artech House Publishers, 2004.

[4] R.C. Olsen, *Remote Sensing from Air and Space*, SPIE Press Monograph Volume 162, 2007.

[5] M. Soumekh, *Synthetic Aperture Radar Signal Processing with MATLAB Algorithms*, Wiley Interscience, 1999.

[6] G. Franceschetti and R. Lanari, *Synthetic Aperture Radar Processing*, CRC Press LCC, 1999.

[7] M. I. Skolnik, *Introduction to Radar Systems*, McGraw-Hill Book Company, New York, 2002.

[8] I. G. Cumming and F. H. Wong, *Digital Processing of Synthetic Aperture Radar Data*, Artech House, Boston, 2003.

[9] W. Palm, *Introduction to Matlab 7 for Engineers*, McGraw Hill, 2004.

[10] *ENVI 4.2 User's Guide Volume 2*, ITT Visual Information Solutions, 2005.

THIS PAGE INTENTIONALLY LEFT BLANK

INITIAL DISTRIBUTION LIST

1. Defense Technical Information Center
   Ft. Belvoir, Virginia

2. Dudley Knox Library
   Naval Postgraduate School
   Monterey, California